



อิทธิพลของ Mn_3O_4 ที่มีต่อสมบัติทางฟิสิกส์ของตัวนำยวดยิ่ง Y145
ซึ่งเตรียมด้วยวิธีปฏิกิริยาสถานะของแข็ง

INFLUENCE OF Mn_3O_4 COMPOSITION ON SOME PHYSICAL PROPERTIES
OF Y145 SUPERCONDUCTOR PREPARED BY SOLID-STATE REACTION

ANONGDAVONE PONCHANTHAI

Graduate School Srinakharinwirot University

2019

อิทธิพลของ Mn_3O_4 ที่มีต่อสมบัติทางฟิสิกส์ของตัวนำยวดยิ่ง Y145
ซึ่งเตรียมด้วยวิธีปฏิกิริยาสถานะของของแข็ง



ปริญญานิพนธ์นี้เป็นส่วนหนึ่งของการศึกษาตามหลักสูตร
การศึกษามหาบัณฑิต สาขาวิชาฟิสิกส์
คณะวิทยาศาสตร์ มหาวิทยาลัยศรีนครินทรวิโรฒ
ปีการศึกษา 2562
ลิขสิทธิ์ของมหาวิทยาลัยศรีนครินทรวิโรฒ

INFLUENCE OF Mn_3O_4 COMPOSITION ON SOME PHYSICAL PROPERTIES
OF Y145 SUPERCONDUCTOR PREPARED BY SOLID-STATE REACTION



A Thesis Submitted in partial Fulfillment of Requirements
for MASTER OF EDUCATION (Physics)
Faculty of Science Srinakharinwirot University

2019

Copyright of Srinakharinwirot University

THE THESIS TITLED

INFLUENCE OF Mn_3O_4 COMPOSITION ON SOME PHYSICAL PROPERTIES
OF Y145 SUPERCONDUCTOR PREPARED BY SOLID-STATE REACTION

BY

ANONGDAVONE PONCHANTHAI

HAS BEEN APPROVED BY THE GRADUATE SCHOOL IN PARTIAL FULFILLMENT OF
THE REQUIREMENTS FOR THE MASTER OF EDUCATION IN PHYSICS
AT SRINAKHARINWIROT UNIVERSITY

Dean of Graduate School

.....
(Assoc. Prof. Dr. Chatchai Ekpanyaskul, MD.)
.....

ORAL DEFENSE COMMITTEE

..... Major-advisor

(Assoc. Prof. Dr. Pongkaew Udomsamuthirun)

..... Chair

(Asst. Prof. Dr. Supphadate
Sujinnapram)

..... Committee

(Dr. Surawut Wicharn)

Title INFLUENCE OF Mn_3O_4 COMPOSITION ON SOME PHYSICAL PROPERTIES OF Y145 SUPERCONDUCTOR PREPARED BY SOLID-STATE REACTION

Author ANONGDAVONE PONCHANTHAI

Degree MASTER OF EDUCATION

Academic Year 2019

Thesis Advisor Associate Professor Dr. Pongkaew Udomsamuthirun

In this research, the Y145 superconductors doping on Mn_3O_4 with the various concentrations of $x = 0, 0.005, 0.010$ and 0.015 are synthesized by the solid-state reaction. The materials of $Y_2O_3, BaCO_3, CuO$ and Mn_3O_4 are mixed, ground and reacted into the two different processes. The physical properties of samples are found that the $YBa_4Cu_5Mn_2O_y$ samples from the powder reacted process had a critical temperature onset at 92 K, 97 K, 95 K and 101 K, respectively. For the composite material process has a critical temperature onset of Y145 + xMn_3O_4 samples as 91 K, 95 K, 92 K and 97 K, respectively. The amount of Mn_3O_4 doped at 0.015 has the highest critical temperature in the initial process. The Mn_3O_4 doping is probably an improvement in morphology; larger grain size and less porosity than the samples without doping. The compositions of elements also demonstrated the uneven distribution of elements, non-homogeneous material and orthorhombic crystal structure. Also, the highest critical temperature in the $YBa_4Cu_5Mn_{0.06}O_y$ sample with Cu^{3+}/Cu^{2+} is equal to 0.222 and the lowest critical temperature is shown in pure $YBa_4Cu_5O_y$ sample with Cu^{3+}/Cu^{2+} equal to 0.170. The results are revealed that the higher the Cu^{3+}/Cu^{2+} ratio is, the higher the critical temperature becomes.

Keyword : Superconductor, Y145 doped with Manganese Oxide, Critical temperature

ACKNOWLEDGEMENTS

I would like to appreciate my sincere gratitude to my major-advisor Assos. Prof. Dr. Pongkaew Udomsamuthirun for the continuous support of my master's study and research, for his patience, motivation, enthusiasm and immense knowledge. His meaningful guidance helped me in all the time of research and writing of this thesis. I could not have imagined having a better major-advisor and mentor for my master's study.

Besides my major-advisor, I would like to express the rest of my thesis committee: Asst. Prof. Dr. Jaturong Sukonthacmat, Asst. Prof. Dr. Chokchai Puttharugsa, Dr. Suwan Plaipichit, Dr. Surawut Wicharn and Asst. Prof. Dr. Supphadate Sujinnapram, for their encouragement, insightful comments and hard questions.

I would like to thank my laboratory staff, Mr. Tunyanop Nilkamjon, Mr. Wirat Wongphakdee, Ms. Somporn Tiyasri and my labmate, Mr. Pariwat Kumtha, for the stimulating discussions and sharing the experience knowledge.

I am exceedingly grateful to the financial support of the center, Department of Physics, Faculty of Science, Srinakharinwirot University for providing really useful experiments and helpful suggestions.

I would like to thank the financial support of the Thailand International Cooperation Agency (TICA), so I would be much obliged.

Finally, I most gratefully acknowledge my family and my friends for all their support throughout the period of this research.

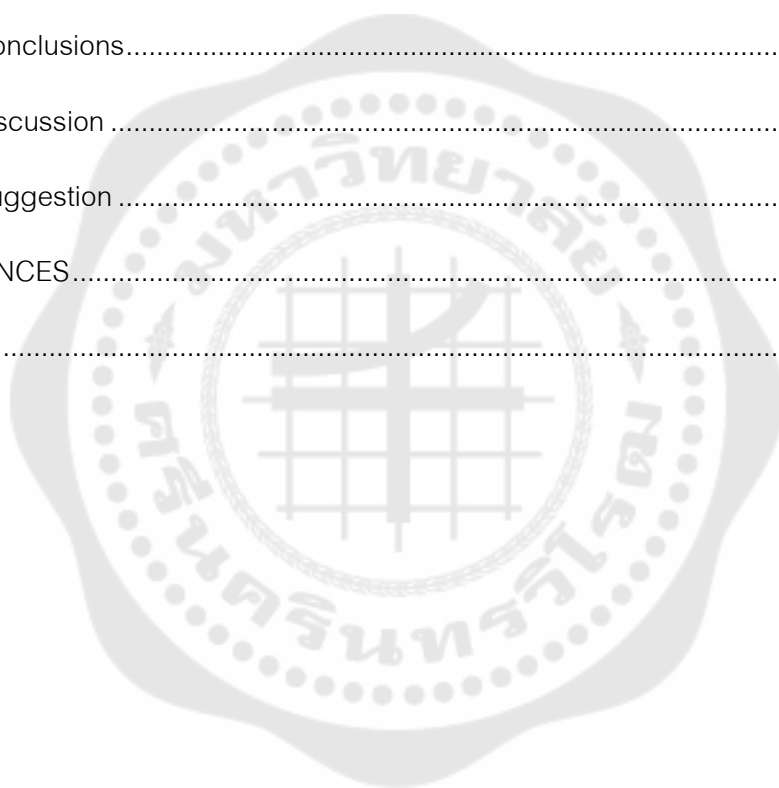
ANONGDAVONE PONCHANTHAI

TABLE OF CONTENTS

	Page
ABSTRACT	D
ACKNOWLEDGEMENTS.....	E
TABLE OF CONTENTS.....	F
LIST OF TABLES.....	I
LIST OF FIGURES	J
CHAPTER 1 INTRODUCTION	1
1.1 Historical background.....	1
1.2 The purpose of the research	5
1.3 The importance of the research.....	5
1.4 Scope of the research.....	6
1.5 Expected benefits from research	6
1.6 The definition of research	6
CHAPTER 2 LITERATURE REVIEW.....	8
2.1 Theory	8
2.1.1 Ginzburg-Landau theory	8
2.1.2 BCS theory.....	10
2.2 The preparation of YBaCuO high-temperature superconductor.....	11
2.2.1 Preparing YBa₂Cu₃O_y (Y123) superconductor	11
2.2.2 Preparing YBa₄Cu₅O_y (Y145) superconductor	14
2.2.3 Preparing YBaCuO superconductor doped with Mn₃O₄	15
2.3. Measuring the electrical resistance.....	16

2.3.1 Four-point probe method	16
2.3.2 Van der Pauw resistivity measurement	18
2.3.3 The Scanning Electron Microscopy	20
2.3.4 Energy-Dispersive X-ray Spectroscopy	21
2.3.5 The X-ray diffraction	23
CHAPTER 3 RESEARCH METHODOLOGY	25
3.1 The preparation of YBaCuO superconductors	26
3.1.1 Preparing Y123 superconductor.....	26
3.1.2 Preparing Y145 superconductor doped with Mn₃O₄	27
3.2 The synthesis of Y145 superconductor doped with Mn₃O₄	30
3.3 Measurement procedure	35
3.3.1 The Electrical Resistance measurement.....	35
3.3.2 Making the probe and measuring the electrical resistance	35
3.3.3 Measuring resistance of the van der Pauw method	36
3.4 Iodometric Titration	37
CHAPTER 4 RESEARCH RESULTS	45
4.1 Resistivity measurements	45
4.1.1 Critical temperature of powders reacted	46
4.1.2 Critical temperature of composite material.....	48
4.1.3 Critical temperature of all samples	50
4.2 Scanning Electron Microscopic (SEM)	54
4.2.1 SEM of powders reacted.....	54
4.2.2 SEM of composite materials.....	59

4.3 Energy-dispersive X-ray spectroscopy	64
4.3.1 EDX of powders reacted	64
4.3.2 EDX of composite materials	66
4.4 The X-ray diffraction	68
4.5 Iodometric titration	69
CHAPTER 5 CONCLUSIONS DISCUSSIONS AND SUGGESTIONS	72
5.1 Conclusions	72
5.2 discussion	74
5.3 Suggestion	76
REFERENCES	77
VITA	81



LIST OF TABLES

	Page
Table 1 Calculating powders of Y145 and Mn₃O₄	29
Table 2 Calculating Y145 superconductor doped with Mn₃O₄	30
Table 3 The titration results of Y123 superconductor	43
Table 4 Variation of normal state and superconducting parameter in different doped samples	47
Table 5 Variation of normal state and superconducting parameter in different doped samples	49
Table 6 Variation of normal state and superconducting parameter in different samples	51
Table 7 This is the variation of doping and the critical temperature onset of samples. ..	53
Table 8 The amount of the elements in many positions	64
Table 9 The amount of the elements in many positions (Continued)	65
Table 10 The ratio of elements in the comparison with yttrium	65
Table 11 The amount of the elements in many positions	66
Table 12 The amount of the elements in many positions (Continued).	67
Table 13 The ratio of elements in the comparison with yttrium	67
Table 14 This is the oxygen content and deficiency of samples.	70

LIST OF FIGURES

	Page
Figure 1 The resistance of mercury sample at low-temperature	2
Figure 2 The Meissner effect T_C	3
Figure 3 The relationship between the internal and external fields of Type I Superconductors	9
Figure 4 The relationship between the internal and external fields of Type II superconductors	10
Figure 5 Lattice deformation when electrons move into the lattice and interact with the lattice	11
Figure 6 Crystal structure of $YBa_2Cu_3O_7$	12
Figure 7 Measuring four-point probe	17
Figure 8 Determination of T_C	17
Figure 9 Van der Pauw resistivity measurements	18
Figure 10 Plot of f versus Q	20
Figure 11 Schematic diagram of the core components of an SEM microscope.	21
Figure 12 Energy-Dispersive X-ray Spectroscopy	22
Figure 13 X-ray diffraction in crystal structure	24
Figure 14 The procedure of research	25
Figure 15 The precursor powders of the sample preparation.....	31
Figure 16 Mixed and ground powder process	31
Figure 17 Calcination process for $YBa_4Cu_5O_y$	32
Figure 18 The calcined powders	32

Figure 19 The pellets sample of $\text{YBa}_4\text{Cu}_5\text{O}_y$	33
Figure 20 Sintering and annealing of $\text{YBa}_4\text{Cu}_5\text{O}_y$ doped with Mn_3O_4	33
Figure 21 The synthesis procedure in the solid-state reaction technique.	34
Figure 22 Equipment for measuring the electrical resistance of a superconductor	36
Figure 23 Van der Pauw measurement structure	37
Figure 24 Resistivity dependence on the temperature for all powder reacted samples .	46
Figure 25 Show the normalized resistivity and the temperature of all powder reacted samples	46
Figure 26 Resistivity dependence on the temperature for all composite material samples	48
Figure 27 Show the normalized resistivity and the temperature of all composite material samples	48
Figure 28 Comparison between the powders reacted and the composite materials samples	50
Figure 29 Shows the normalized of the powders reacted and the composite materials samples	50
Figure 30 The concentrations versus the critical temperature onset	52
Figure 31 SEM photographs of $\text{YBa}_4\text{Cu}_5\text{O}_y$ at the power magnifications a) 500, b) 1000 and c) 2000	55
Figure 32 SEM photographs of $\text{YBa}_4\text{Cu}_5\text{Mn}_{0.015}\text{O}_y$ at the power magnifications a) 500, b) 1000 and c) 2000	56
Figure 33 SEM photographs of $\text{YBa}_4\text{Cu}_5\text{Mn}_{0.03}\text{O}_y$ at the power magnifications a) 500, b) 1000 and c) 2000	57
Figure 34 SEM photographs of $\text{YBa}_4\text{Cu}_5\text{Mn}_{0.06}\text{O}_y$ at the power magnifications a) 500, b) 1000 and c) 2000	58

Figure 35 SEM photographs of Y145 at the power magnifications a) 500, b) 1000 and c) 2000	60
Figure 36 SEM photographs of Y145 + 0.005 Mn ₃ O ₄ at the power magnifications a) 500, b) 1000 and c) 2000	61
Figure 37 SEM photographs of Y145 + 0.010 Mn ₃ O ₄ at the power magnifications a) 500, b) 1000 and c) 2000	62
Figure 38 SEM photographs of Y145 + 0.015 Mn ₃ O ₄ at the power magnifications a) 500, b) 1000 and c) 2000	63
Figure 39 The X-ray diffraction patterns of samples in the powders reacted process....	68
Figure 40 The X-ray diffraction patterns of samples in the composite materials process.	69
Figure 41 This is the effect of two processes and oxygen deficiency on the critical temperature onset of all samples.....	71
Figure 42 Shows the ratio of Cu ³⁺ /Cu ²⁺ versus the critical temperature onset.....	71

CHAPTER 1

INTRODUCTION

1.1 Historical background

The studies on superconductors have been conducted for a long time. Those results established a new branch of knowledge and technological development in scientific communities. The interesting things about superconductors are the applications of materials in engineering fields. The superconductors are a material which absent of direct current resistance. The superconductors are created as imaging equipment in the Magnetic Resonance Imaging (MRI). MRI is perhaps the best application of superconductivity which directly has an impact on humans all over the world. It is a common tool with the radiologist in diagnostic hospitals for imaging various soft tissue parts of the human body and for detecting tumors. These devices are capable to generate detailed images of internal structures. In addition, the superconductors also used to develop a powerful magnetic particle accelerator in the Large Hadron Collider (LHC) because of losing energy in the form of heat when a high current flowing through. Moreover, superconductors are also generated in a magnetic field in the Magnetic Levitation train (Maglev) which the superconductors are made to float over magnets when it is in the coolant. However, the superconductors still face a restriction in applications such as it has to operate at a low temperature and so on. It has seen that more crucial information required for developing a highly effective superconductor and applying widely to other fields.

In 1908, Heike Kammerlingh Onnes, a Dutch physicist, liquefied helium to a temperature below 4.2 K . Onnes applied his newly found coolant to mercury and measured the electrical resistance through the super cooled element. The results from this experiment showed that resistivity decreased in the mercury under the influence of liquid helium. Subsequently, Onnes found that the electrical resistivity of many metals and alloys drops suddenly to zero when the specimen is cooled to a sufficiently low temperature. So, he called the new phenomenon, "superconductivity"(Buckel, 1991).

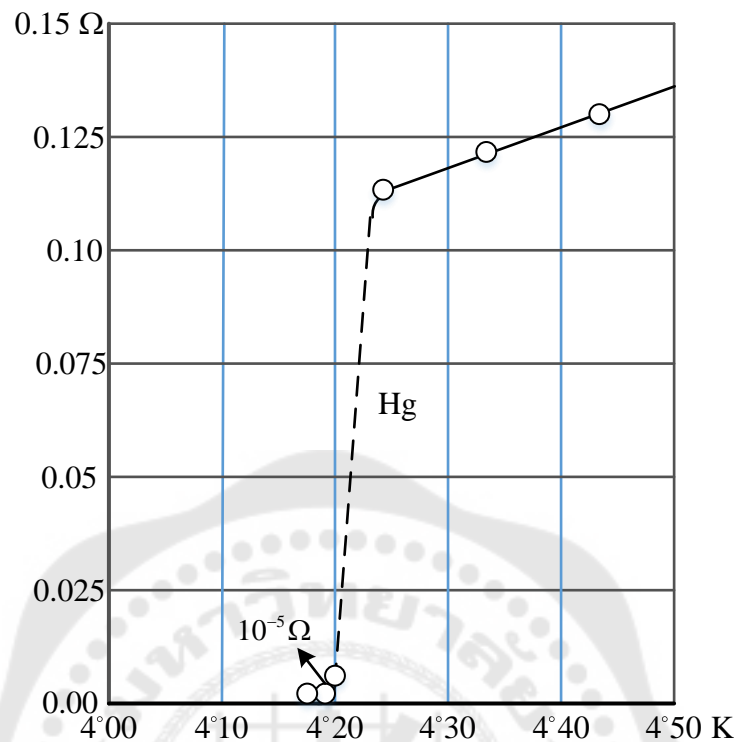


Figure 1 The resistance of mercury sample at low-temperature

Source: Kittel, C. (1962). *Elementary solid state physics : a short course*: New York : Wiley. p.258.

An elementary property of superconductivity as observed by Onnes that the superconducting state may be destroyed by placing the sample in the strong magnetic field. Furthermore, superconductivity reappears when the field is removed and the field strength required to destroy the superconducting state depends on the orientation of the specimen within the field. Onnes had discovered superconductivity and was awarded the Nobel Prize in 1913.

In 1933, the experiments by Walther Meissner and Robert Ochsenfeld (Omar, 1975, p. 500) found that superconductors have more properties than a perfect conductor, they also have an interesting magnetic property of excluding a magnetic field. A superconductor will not allow a magnetic field to penetrate its interior. This effect called "the Meissner effect", make happen a phenomenon that is a very popular demonstration of superconductivity. The Meissner effect will take place only if the

magnetic field is relatively small. If the magnetic fields are higher than the critical magnetic field, the metal loses its superconductivity

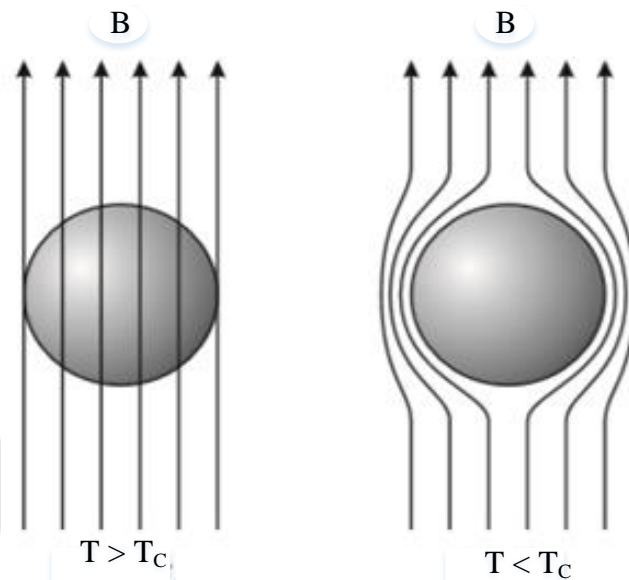


Figure 2 The Meissner effect T_c

Source: Laphorn, A.; Bodger, P.; & Enright, W. (2013). A 15-Kva High-Temperature Superconducting Partial-Core Transformer-Part 1: Transformer Modeling. *IEEE Transactions on Power Delivery*. 28(1): 245-252. p.18.

In 1986, when Alex Muller and Georg Bednorz (Bednorz & Müller, 1986) researchers at an IBM laboratory in Switzerland, discovered that ceramics from a class of materials called perovskites were superconductors at the temperature of about **30 K**. The superconductivity was found in **BaLaCuO** system in **30 K** range. This event sparked great excitement in the world of physics and earned the Nobel Prize in Physics in 1987. As a result of this breakthrough, scientists began to examine the various perovskite materials very carefully. In February of 1987, they found that the ceramic material was a superconductor at **90 K**. This was very significant because now it became possible to use liquid nitrogen as the refrigerant. Since these material superconductors at a significantly higher temperature, they are called “high-temperature superconductors”.

The following year, researchers (Wu et al., 1987) from the University of Alabama and Houston using yttrium instead of lanthanum were able to observe superconductivity transition at **80 K–93 K**. These materials came to be as high-temperature superconductors due to their greatly increased critical temperature. This discovery was important because liquid nitrogen could then be used as a coolant instead of liquid helium. The nitrogen has a boiling point of **77 K** at atmospheric pressure and is cheap and easy to produce from the atmosphere thus avoiding some of the expenses associated with liquid helium.

Udomsamuthirun and co-workers (2010), found the new **YBaCuO** superconductors of materials. They synthesized by using the standard solid-state reaction method as compositions of **Y5-6-11**, **Y7-9-16**, **Y358**, **Y5-8-13**, **Y7-11-18**, **Y156**, **Y3-8-11**, and **Y13-20-23**, where the numbers denote **Y**, **Ba**, and **Cu** atoms respectively. A few years, Chainok et.al (2013) studied the **YBaCuO** superconductors having one yttrium atom that **Y123**, **Y134**, **Y145** and **Y156**. The sintering temperature at **950 °C** and **980 °C** were used for synthesized their samples. The critical temperature in range **88 K- 94 K** was found. Some properties of **Y145** superconductor has been re-examined by comparing to **Y123** that the preparing process were solid-state reaction and melt process. The critical temperature onset of **Y145** at **94 K** and **96 K** for solid-state reaction and melt process were found, respectively. Supadanaison et.al (2018) studied some properties of **Y134** and **Y145** superconductor. These superconductors doped with Ag_2O were synthesized by solid-state reaction.

Salama et al. (2015) studied the effect of magnetic and nonmagnetic superconductor samples of **YBaCuO** doped with nano metal oxides of Mn_3O_4 , Co_3O_4 , Cr_2O_3 , **CuO** and Sn_2O_3 respectively with **0.2 wt%** are synthesized by a solid-state reaction route. Next year, Salama et al. (2016) investigated the influence of magnetic nano metal oxides. The superconductor samples of **YBaCuO + x** where $x = 0.1, 0.2, 0.3, 0.4$ and **0.5 wt%** of nano metal oxides namely Cr_2O_3 , Co_3O_4 and Mn_3O_4 were synthesized by the solid-state reaction route.

In this research, we modified the influence superconductor sample of **Y145** ($\text{YBa}_4\text{Cu}_5\text{O}_y$) doped with Mn_3O_4 by using the solid-state reaction method. The raw materials Y_2O_3 , BaCO_3 and CuO were mixed, ground and reacted, respectively. The crystal structures of samples were investigated by using X-ray diffraction (XRD). The surfaces of materials were taken by scanning electron microscopy (SEM). The identification of the composition of different elements in the specific samples were determined by using the energy-dispersive X-ray spectroscopy (EDX). The Iodometric titration are used to determine the amount of Cu^{2+} , Cu^{3+} and oxygen content. The resistivity measurements and the critical temperature were measured by using the four-point probe method. Recently, many researchers obviously reported that the **YBaCuO** superconductors doped with Mn_3O_4 can be increased T_c significantly which is attributed to the inclusion of **Mn** reducing the formation of other **Y-123** phases and enhancing the formation of **YBaCuO** with high orthorhombicity and high superconductor properties.

1.2 The purpose of the research

1. To study the preparation process of Y_2O_3 , BaCO_3 , CuO ,and Mn_3O_4 precursor powders by solid-state reaction:

1.1 The powders reacted $\text{Y}_2\text{O}_3 + \text{BaCO}_3 + \text{CuO} + (x)\text{Mn}_3\text{O}_4$

1.2 The composite material $\text{YBa}_4\text{Cu}_5\text{O}_y + (x)\text{Mn}_3\text{O}_4$

2. To study the critical temperature by four-point probe resistivity measurement.

3. To study the physical properties of the powders reacted and the composite materials of superconductor doped with Mn_3O_4 including the X-ray diffraction (XRD), the energy-dispersive X-ray spectroscopy (EDX), the scanning electron microscopy (SEM) and the iodometric titration.

1.3 The importance of the research

1. comprehending the preparation process and the measurement processes in the physical properties of the powders reacted and the composite materials of superconductor doped with Mn_3O_4 .

2. comprehending the phenomenon of superconductivity that occurs in the critical temperature and to realize the value of critical temperature.

1.4 Scope of the research

1. To prepare the powders (Y_2O_3 , BaCO_3 , CuO and Mn_3O_4) reacted and the composite materials of superconductor doped with Mn_3O_4 by solid-state reaction.

2. To know the critical temperature by four-point probe resistivity measurement.

3. To investigate the physical properties of the powders reacted and the composite materials of superconductor doped with Mn_3O_4 including the X-ray diffraction (XRD), the energy-dispersive X-ray spectroscopy (EDX), the scanning electron microscopy (SEM) and the iodometric titration.

1.5 Expected benefits from research

1. To understand the preparation process of the powders reacted and the composite materials of superconductor doped with Mn_3O_4 by solid-state reaction.

2. To see the structure and the physical properties of the powders reacted and the composite materials of superconductor doped with Mn_3O_4 .

3. To guide in the synthesis process of other YBaCuO superconductors.

1.6 The definition of research

Solid-state reaction: is the most widely used method for the preparation of crystalline solids from a mixture of solid starting materials. Solids do not react together at room temperature over normal time scales and it is necessary to heat them higher temperature and to create the reaction to be a crystal structure.

Powders reacted: is the mixing of precursor powders process. There are Y_2O_3 , BaCO_3 , CuO and Mn_3O_4 powders which are doped by the different concentrations.

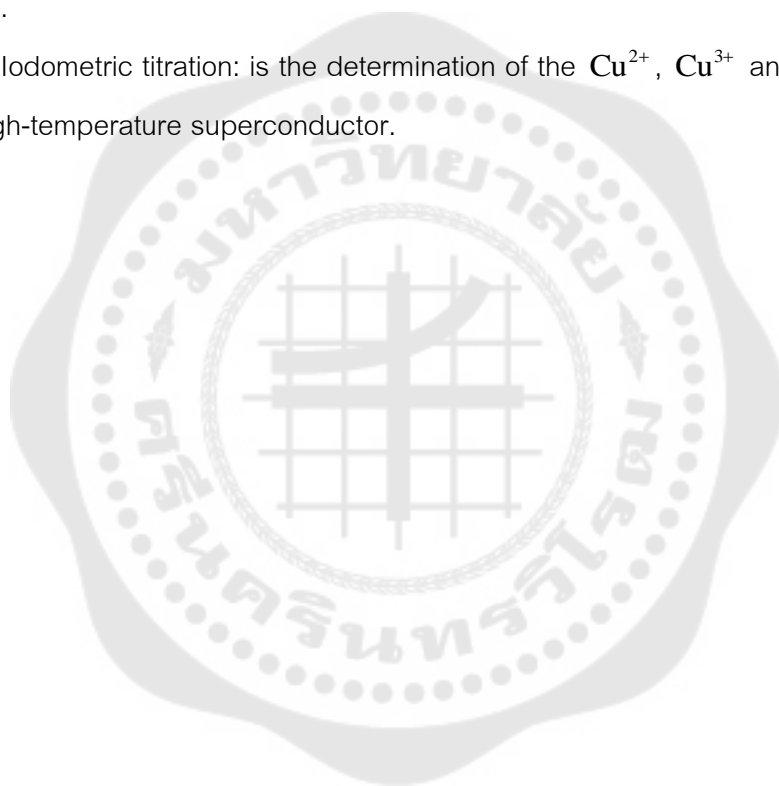
Composite material: is the process of $\text{YBa}_4\text{Cu}_5\text{O}_y$ superconductors doped with Mn_3O_4 by the different concentrations.

Calcination: is the calcining process of compound solid in high temperature which starts at 100°C – 950°C for making the compound to react the adhesion in the crystalline structure.

Sintering: is the sintering process to start at 100°C – 950°C for creating the reaction material bond together into a strong crystalline structure.

Annealing: is the heat treatment process annealed at 550°C for 24 hours in the air. This process is the absorption and discharging of some oxygen into the crystalline structure.

Iodometric titration: is the determination of the Cu^{2+} , Cu^{3+} and oxygen content in the high-temperature superconductor.



CHAPTER 2

LITERATURE REVIEW

In this research, we study the influence of Mn_3O_4 composition on some physical properties of **Y145** superconductor prepared by solid-state reaction. There are theories of the superconductor, preparations process, measurement process, SEM, EDX, and XRD, respectively. These will be discussed in further detail.

2.1 Theory

2.1.1 Ginzburg-Landau theory

In 1950, Ginzburg-Landau presented the theory of Ginzburg-Landau that is the system macroscopic theory. To explain the property of superconductor in a magnetic field such as phase transition of superconductor from the normal state to be the superconducting state at the critical temperature. By the initial concept of this theory derived from the determination to the system of superconductivity which is the variation of the order parameter. Later, the Ginzburg-Landau theory was identified to classify the new superconductors using the relationship between the coherent length, ξ and the London penetration depth. To determine the Ginzburg-Landau parameter, K which is the ratio between the London penetration depth and coherent length as $K = \lambda_L / \xi$, which can be divided into two types of superconductors. The Type I Superconductors is the value of the Ginzburg-Landau parameter, K less than $1/\sqrt{2}$ and the Type II Superconductors is the value of the Ginzburg-Landau parameter, K greater than $1/\sqrt{2}$ (Fetter & Walecka, 2012).

In general, high temperatures and high magnetic fields destroy the superconductivity. If the temperature is less than critical temperature and superconductors are called Type I Superconductors the following relationship between the internal and external fields is as Figure 3.

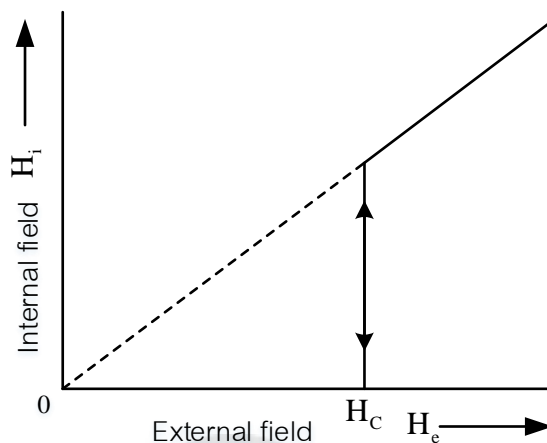


Figure 3 The relationship between the internal and external fields of Type I Superconductors

Source: Buckel, Werner. (1991). *Superconductivity: Fundamentals and Applications*. Weinheim: VCH. p.211

For external fields higher than critical fields, we have the normal state which is assumed to be nonmagnetic ($H_i = H_e$). For the external fields less than critical fields, we have the Meissner effect ($H_i = 0$).

For Type II superconductors, the degree of flux penetration is according to the following diagram in Figure 4. There are two critical magnetic fields in Type II superconductors, H_{C1} and H_{C2} . For $H > H_{C2}$, the sample is normal state $H_i = H_e$, whilst for $H < H_{C1}$, the samples are complete Meissner effect ($H_i = 0$). In the intermediate state $H_{C1} < H_e < H_{C2}$, the sample is in a mixed condition with non-uniform flux penetration. H_{C1} and H_{C2} are called the lower and upper critical fields, respectively.

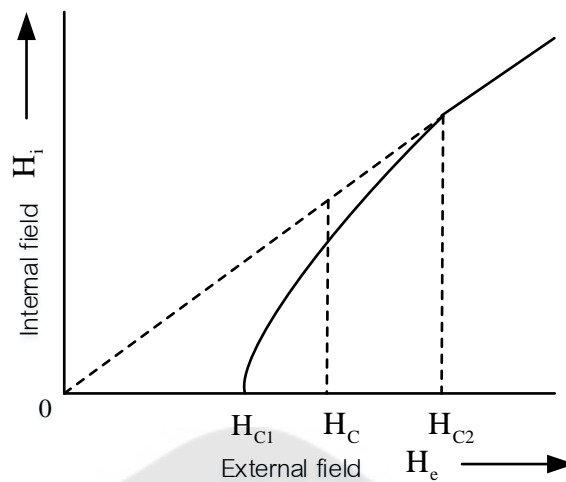


Figure 4 The relationship between the internal and external fields of Type II superconductors

Source: Buckel, Werner. (1991). *Superconductivity: Fundamentals and Applications*. Weinheim : VCH. p.235

2.1.2 BCS theory

In 1957, BCS theory was proposed by Bardeen, Cooper, and Schrieffer (1957, p. 1175) BCS is the microscopic theory that can explain the superconductivity in the superconducting substances with low critical temperature. To describe the important mechanism of this theory that enables the normal conductor to superconductors are the capture pairs of electrons called the Cooper Pairs. When electrons move into the lattice, they interact with the crystal lattice structure and then creates crystal lattice deforming as shown in Figure 5. This interaction is an electron-lattice-electron interaction, when electrons move through the group of ions with the positive charge on the lattice. Electrons will attract positive ions in the surrounding areas and deform the lattice around it. The density of the positive ions increases and then attracts other electrons. As a result, it seems that two electrons effectively attract each other. The pairing of the electron made it lose some energies. It causes an energy gap at the Fermi surface in the

superconductor. The superconductors that obey the BCS theory are called s-wave superconductors.

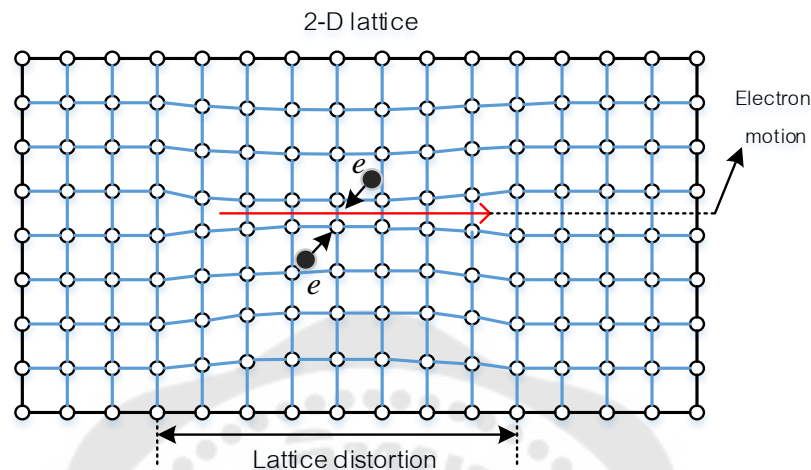


Figure 5 Lattice deformation when electrons move into the lattice and interact with the lattice

Source: Sharma, R.G. (2015). *Superconductivity*. Cham: Springer. Retrieved from 28/03/2019 <http://www.bookmetrix.com/detail/book/b8daf2d7-9419-4516-bb81-c399ddb667ab#citations>. p 118.

2.2 The preparation of YBaCuO high-temperature superconductor

2.2.1 Preparing $\text{YBa}_2\text{Cu}_3\text{O}_y$ (Y123) superconductor

Wu et.al (1987) discovered superconductivity in a $\text{YBa}_2\text{Cu}_3\text{O}_y$ (or simply YBCO or also called just Y123) system at 93 K making it possible first time to cool down a superconductor below its T_C using liquid nitrogen instead of liquid helium. The most popular technique for preparing Y123 is the standard technique of solid-state reaction route. Appropriate quantities of Y_2O_3 , BaCO_3 and CuO .

The superconducting phase was identified to be $\text{YBa}_2\text{Cu}_3\text{O}_7$ which is an oxygen-deficient triplet perovskite unit cell of the type ABX_3 . $\text{YBa}_2\text{Cu}_3\text{O}_7$ has an orthorhombic distorted structure and is shown in Figure 6. clearly Cu ion has two distinct crystallographic and dissimilar sites Cu(1) and Cu(2). Cu(1) is surrounded

by a squashed square planar O configuration in the b-c plane and linked to similar sites in a one dimension along the b-axis. Cu(2) site is 5 coordinated by a square pyramidal arrangement of O. the vertex of the pyramid is at O(4) site along the c-axes. The Y ion is at the center of the two Cu-O sheets eight O-coordinated and Ba ten O-coordinated. We thus find that Cu-O network is important for cuprates. Cu(1)-O(1) chains are crucial to superconductivity in this material. Cu(2)-O(2)/O(3) do not seem to be so crucial for 90 K transitions. Cu(1)-O(4) bond is much stronger than Cu(1)-O(1), bond lengths being 1.850\AA and 1.943\AA , respectively. Oxygen vacancies occur in O(1) site easy which brings down the transition temperature. At stoichiometric O_7 , cooper exists in the divalent and trivalent state as per the expression below:

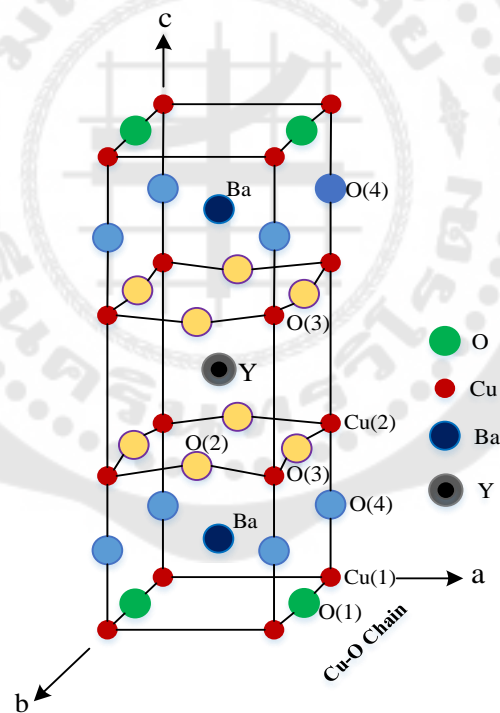
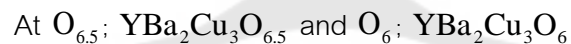


Figure 6 Crystal structure of $\text{YBa}_2\text{Cu}_3\text{O}_7$

Source: Sharma, R.G. (2015). *Superconductivity*. Cham: Springer. Retrieved from 28/03/2019 <http://www.bookmetrix.com/detail/book/b8daf2d7-9419-4516-bb81-c399ddb667ab# citations>. p. 78.

Oxygen depletion leads to a change in structure orthorhombic to tetragonal. T_C starts decreasing with oxygen loss and changes the oxidation state of **Cu**. As O content decreases from 7 to 6.5, T_C decreases from 93 K to 55 K. **Cu(1)** and **Cu(2)** are in divalent state. At $O = 6.5$ the material becomes semiconducting. In fact, there is a plateau in the T_C versus O-content curve at $O_{6.5}$. As O-content decreases further, T_C decreases too and at $O = 6$, the material turns into an insulator. The oxidation state of **Cu** reduces to univalent the oxidation states of **Cu** at O_6 and $O_{6.5}$ can be expressed like this:



The simplest method for preparing the **Y123** superconductor is an important technique for synthesizing perovskite ceramic. So, there is the same preparation form as general ceramics and there are some different details to create a unique property of this group. There is 3 major heating process.

1) The calcination is the process of calcined the powder to make the substance react with the adhesion of the structure and to make the elements of the unwanted substance away. In the case of the **YBaCuO** superconductor, the heating process will make the substance to form aggregates and will be the structure of a compound. This calcination process is at around $800\text{-}1100^\circ\text{C}$.

2) The sintering is a process of sintered by beginning from the pellets and sintering at appreciate temperature. To create the reaction material bond together into a strong compound structure. For the **YBaCuO** superconductor is sintered at $800\text{-}1100^\circ\text{C}$ for 24 hours.

3) The annealing is a process of absorbing and discharging some oxygen into and out of the structure of the compound. The simple of **YBaCuO** superconductor is annealed at around $400\text{-}550^\circ\text{C}$.

Kruaehong et al. (2018) prepared and synthesized of superconductor **YBaCuO** by using the solid-state reaction method. There are the powders of Yttrium Oxide (Y_2O_3), Barium Carbonate (BaCO_3) and Copper Oxide (**CuO**). To calculate a ratio of the substrate according to the chemical formula of **Y123** superconductor is



Ceramic superconducting sample of Y123 is synthesized by standard solid-state reaction method using raw materials of Y_2O_3 , BaCO_3 , and CuO of high purity (99.99%) in the desired atomic ratio as 1:2:3. When appropriate quantities of Y_2O_3 , BaCO_3 and CuO , as per formula unit $\text{YBa}_2\text{Cu}_3\text{O}_y$ are mixed thoroughly and ground in a pestle mortar. The fine powder prepared is calcined at 950°C for about 24 hours. This powder finely crushed and calcined again. This process is repeated two times when a homogenous mixture is obtained. The powder is then pressed into the form of a pellet and sintered at 950°C for 24 hours under flowing oxygen. It is important to cool the sample slowly from the sintering temperature to have the stoichiometric oxygen in the compound. And then the sample is annealed at 550°C for 24 hours. This process plays a crucial role in the reaction in the air.

2.2.2 Preparing $\text{YBa}_4\text{Cu}_5\text{O}_y$ (Y145) superconductor

Chainok et al. (2013) synthesized and characterized the physical properties of $\text{YBa}_2\text{Cu}_3\text{O}_y$ (Y123) and $\text{YBa}_4\text{Cu}_5\text{O}_y$ (Y145) superconductor by solid-state reaction and melt process. The raw materials Y_2O_3 , BaCO_3 and CuO were mixed, ground and react in the air atmosphere at 950°C , at 980°C . The samples obtained were characterized by the resistivity measurement, SEM, EDX, XRD and DTA. It was found that the critical temperature onset of Y145 is 94 K and 96 K for solid-state reaction and melt process, respectively. The samples were inhomogeneous with no impurity. The crystal structure was orthorhombic which $a = 3.80446 \text{ \AA}$, $b = 3.86474 \text{ \AA}$ and $c = 19.37104 \text{ \AA}$ for Y145 solid-state reaction and $a = 3.80180 \text{ \AA}$, $b = 3.86483 \text{ \AA}$ and $c = 19.38194 \text{ \AA}$ for melt process. The peritectic temperature of Y145 is 1018°C . A few years later (2015), they synthesized the $\text{YBa}_m\text{Cu}_{1+m}\text{O}_y$ superconductors, $m = 2, 3, 4$ and 5 that were Y123 ($\text{YBa}_2\text{Cu}_3\text{O}_{7-x}$), Y134 ($\text{YBa}_3\text{Cu}_4\text{O}_{9-x}$), Y145 ($\text{YBa}_4\text{Cu}_5\text{O}_{11-x}$) and Y156 ($\text{YBa}_5\text{Cu}_6\text{O}_{13-x}$) by solid-state reaction with the Y_2O_3 , BaCO_3 and CuO as the starting materials. The calcination temperature was 950°C

and varied the sintering temperature to be 950°C and 980°C . The resistivity measurement by the four-point probe technique showed that the T_{C} of Y123, Y134, Y145, Y156 were at 97 K, 93 K, 91 K and 85 K, respectively. The XRD and Rietveld full-profile analysis method were used and found that the crystal structure were in the orthorhombic with Pmmm space group with the ratio c/a were 3.0, 4.0, 5.0 and 6.0 for Y123, Y134, Y145, Y156. The oxygen contents were characterized by Iodometric titration. they also found that the increasing of sintering temperature has reduced the oxygen content and the critical temperature of all samples.

Supadanaison et al. (2018) studied the Y145 superconductor doped Ag_2O were synthesized by solid-state reaction. The calcinations and sintering temperature were at 950°C and annealing temperature was at 550°C . The highest critical temperature was in Y145+0.1Ag sample with T_{C} onset at 96 K and the lowest was found in pure Y145 at 95 K. they found that the surface of Y145 superconductor was improved by Ag adding on the porous structure.

2.2.3 Preparing YBaCuO superconductor doped with Mn_3O_4

Salama et al. (2015) studied the effect of magnetic and nonmagnetic nano metal oxides doping on the critical temperature of a YBaCuO superconductor. The bulk superconductor samples of $\text{YBa}_2\text{Cu}_3\text{O}_{7-x}$ (YBaCuO) doped with nano metal oxides of Mn_3O_4 , Co_3O_4 , Cr_2O_3 , CuO and SnO_2 , respectively with 0.2 wt% were synthesized by a solid-state reaction route. The structure characterization of all samples were carried out by X-ray diffraction (XRD) and scanning electron microscopy (SEM) and transmission electron microscopy (TEM) techniques. The XRD patterns indicated that the magnetic doping with nano metal oxides (Mn_3O_4 , Co_3O_4 , Cr_2O_3) gave a high value of orthorhombicity of the YBaCuO samples which was the result of high oxygen content, and consequently could give better superconducting properties contrary to the nonmagnetic nano oxides (CuO , SnO_2). The critical temperature (T_{C}) of the studies samples were found to improve by nano magnetic doping and lower with nano nonmagnetic doping. The superconducting transition temperature T_{C} determined from

electrical resistivity measurements were found to increase for Mn_3O_4 ($5.27 \mu\text{B}$) doping and decrease for other metal oxides doping.

In 2016, Salama et al. (2016) studied the influence of magnetic nano metal oxides doping on structure and electrical properties of YBaCuO superconductor. The superconductor samples of $\text{YBa}_2\text{Cu}_3\text{O}_{7-x}$ (YBCO) + x where $x = 0.1, 0.2, 0.3, 0.4$ and $0.5 \text{ wt}\%$ of nano metal oxides namely Co_3O_4 , Cr_2O_3 and Mn_3O_4 respectively. The X-ray diffraction and electron microscopy were employed to study the phase identification and the microstructure of these samples. Critical temperature of the samples were determined by four probe resistivity measurements. The X-ray diffraction patterns indicated that the gross structure of YBaCuO did not change with the substitution of three types of nano metal oxides with different doping level. The critical temperature (T_C) were found to decrease with the increases of doping level. YBaCuO doped with Mn_3O_4 had the highest T_C value which might be due to flux pinning from some defects and the rapid suppression in T_C with increasing concentration of Mn_3O_4 might be due to the cooper pair breaking and the hole filling in the CuO_2 planes.

2.3. Measuring the electrical resistance

2.3.1 Four-point probe method

The four-point probe is the most common method of determining the T_C of a superconductor. The superconductor is attached to the four-point probe with a conductive adhesive shown in Figure 7. Two of four probes are connected by a voltage and others are linked by current. The current is a constant kept at 200 mA flowing through the superconductor. Then, if resistance exists in the sample, a voltage will appear across the other two points in accordance with Ohm's law. When the sample transits to be a superconducting state, its resistance drops to zero and no voltage. Before measuring the four-point probe, all of the samples are tested by the resistance parameter at room temperature, not more than 10Ω .

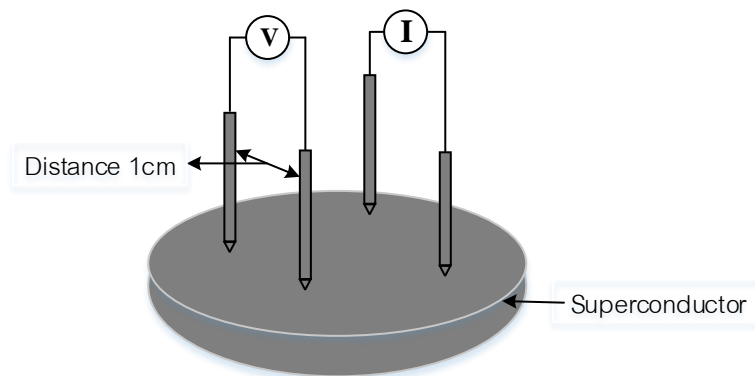


Figure 7 Measuring four-point probe

The critical temperature of a superconductor (Murase et al., 2001) is defined as the temperature below which a superconductor exhibits superconductivity at zero magnetic field strength. In this method, the resistance measurement is performed with the four probe technique and the critical temperature is determined as the mid-point of resistance transition from normal state to superconducting state with minimum of the D.C. transport current (specimen current) and at no applied magnetic field strength except for geomagnetism. Figure 8 shows schematically a curve of resistance versus temperature for a composite superconductor.

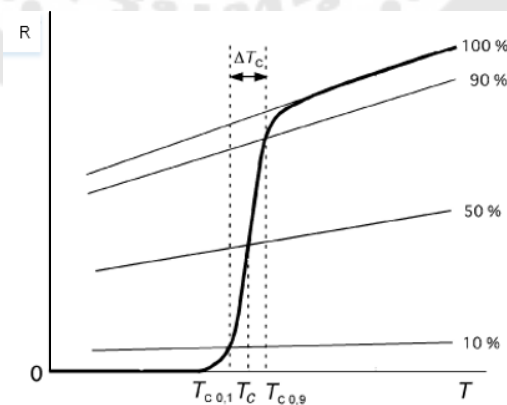


Figure 8 Determination of T_c

Source: Murase, S., Itoh, K., Wada, H., Noto, K., Kimura, Y., Tanaka, Y., & Osamura, K. (2001). Critical temperature measurement method of composite superconductors. *Physica C: Superconductivity*, 357, 1197-1200.

A tangential line to a part of curve in the normal state region can be drawn. The value of temperature at intersection of the transition curve and a line with 50% height of the tangential line (50% resistance) is determined as T_C . Two temperature values at the intersections of the transition curve and two lines with 10% and 90% heights of the tangential line are denoted by $T_{C0.1}$ and $T_{C0.9}$, respectively, as shown in Figure. 8. The transition width, ΔT_C is defined as $T_{C0.9} - T_{C0.1}$. ΔT_C shall be less than 3% of T_C .

2.3.2 Van der Pauw resistivity measurement method

Da luz et al. (2009) investigated the van der Pauw method involve applying a current and measuring voltage using four small contacts on the circumference of a flat, arbitrarily shaped sample of uniform thickness. The method is particularly useful for measuring very small samples because geometric spacing of the contacts is unimportant. Effects due to a sample's size which is the approximate probe spacing, are irrelevant.

Using this method, the resistivity can be derived from a total of eight measurements that are made around the periphery of the sample with the configurations show in Figure 9.

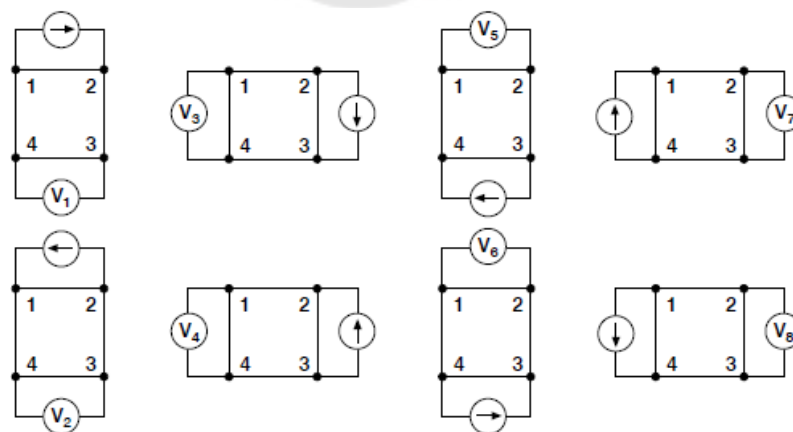


Figure 9 Van der Pauw resistivity measurements

Source: Keithley, J. F. (1984). Low level measurements: for effective low current, low voltage, and high impedance measurements: Keithley Instruments.

Once all the voltage measurements are taken, two values of resistivity, ρ_A and ρ_B , are derived as follows:

$$\rho_A = \frac{\pi}{\ln 2} f_A t_s \frac{(V_1 - V_2 + V_3 - V_4)}{4I} \dots\dots\dots (2.1)$$

$$\rho_B = \frac{\pi}{\ln 2} f_B t_s \frac{(V_5 - V_6 + V_7 - V_8)}{4I} \dots\dots\dots (2.2)$$

When ρ_A and ρ_B are known, the average resistivity can be determined as follows:

$$\rho_{avg} = \frac{\rho_A + \rho_B}{2} \dots\dots\dots (2.3)$$

- Where ρ_A and ρ_B are volume resistivity
- t_s is the sample thickness
- I is the current through the sample
- f_A and f_B are geometrical factors based on sample symmetry

We can find the value of f_A and f_B from calculating the related the two resistance ratios Q_A and Q_B as shown in the following equations ($f_A = f_B = 1$ for perfect symmetry). Also Q and f are related as follows:

$$\frac{Q-1}{Q+1} = \left(\frac{f}{0.693} \right) \arccos \left(\frac{e^{0.693/f}}{2} \right) \dots\dots\dots (2.4)$$

Q_A and Q_B are calculated by using the measured voltages as follows:

$$Q_A = \frac{V_1 - V_2}{V_3 - V_4} \dots\dots\dots (2.5)$$

$$Q_B = \frac{V_5 - V_6}{V_7 - V_8} \dots\dots\dots (2.6)$$

A plot of this function is shown in figure 10. The value of f can be found from this plot once Q has been calculated.

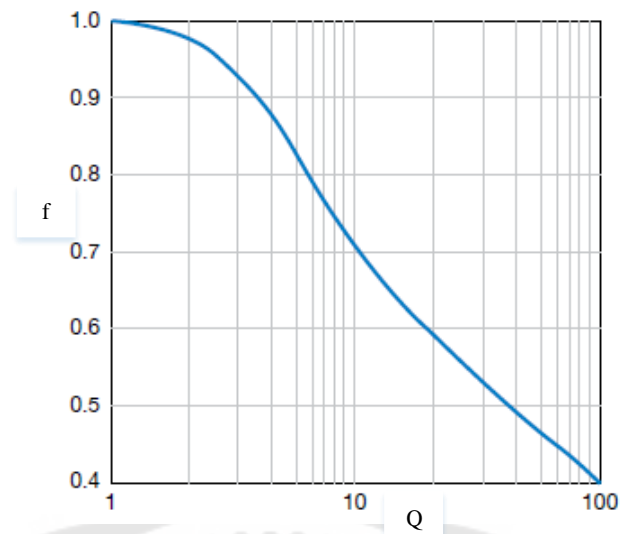


Figure 10 Plot of f versus Q

Source: Keithley, J. F. (1984). *Low level measurements: for effective low current, low voltage, and high impedance measurements*: Keithley Instruments.

2.3.3 The Scanning Electron Microscopy

The scanning electron microscopy (SEM) is the technique of choice for analysis of specimen surfaces. The SEM has a power maximum magnification of about 10 nm. In Figure 11 shows the typical layout of the SEM, which includes the electron gun. The electron gun serves to produce the electron for entering into the system. The electron groups from the source will be accelerated by a magnetic field. Then the electron groups will move through to the condenser lenses. To create the electron groups become the electron beam which is used to focus the electrons into a beam, adjust beam astigmatism, move the beam across the specimen, and to scan the beam to generate images. The electrons move on impacting the surface of the sample which will be created the electrons of the sample ejected into the secondary electron detector. To collect the signals emitted from the specimen analyzed the surface characteristic of a specimen and processed as images displaying on the computer screen.

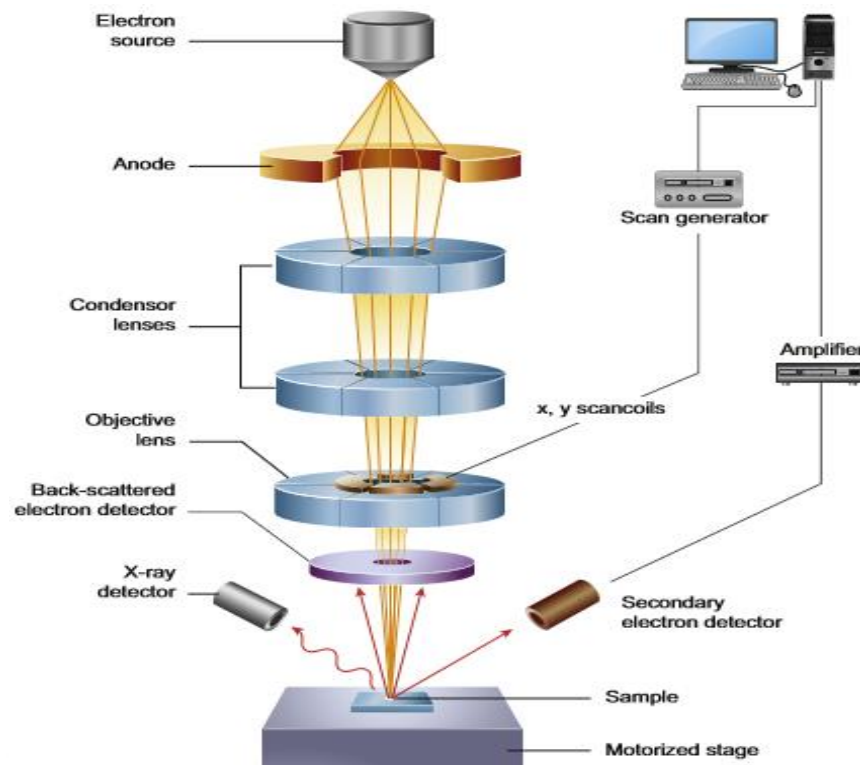


Figure 11 Schematic diagram of the core components of an SEM microscope.

Source: Inkson, B. (2016). Scanning electron microscopy (SEM) and transmission electron microscopy (TEM) for materials characterization *Materials characterization using nondestructive evaluation (NDE) methods* (pp. 17-43): Elsevier.

2.3.4 Energy-Dispersive X-ray Spectroscopy

Energy-dispersive X-ray spectroscopy (EDX) is used to analyze the elemental composition of solid surfaces. It relies on an interaction between some sources of X-ray excitation and a sample. EDX can be used to determine which chemical elements are present in a sample. X-ray emission is stimulated by the irradiation of the surface with a high energy beam of charged particles or a focused X-ray beam. Excitation of the electronic structure of an atom can produce an X-ray emission called the primary X-ray beam. The primary X-ray beam will make the inner electrons of the elemental atom ejected shown Figure 12. Then, the outer electrons with high energy levels will replace and emit excess energy called a secondary X-ray beam.

The secondary X-ray beam has a special value of that material which is used in quantitative analysis and type of elements in the sample.

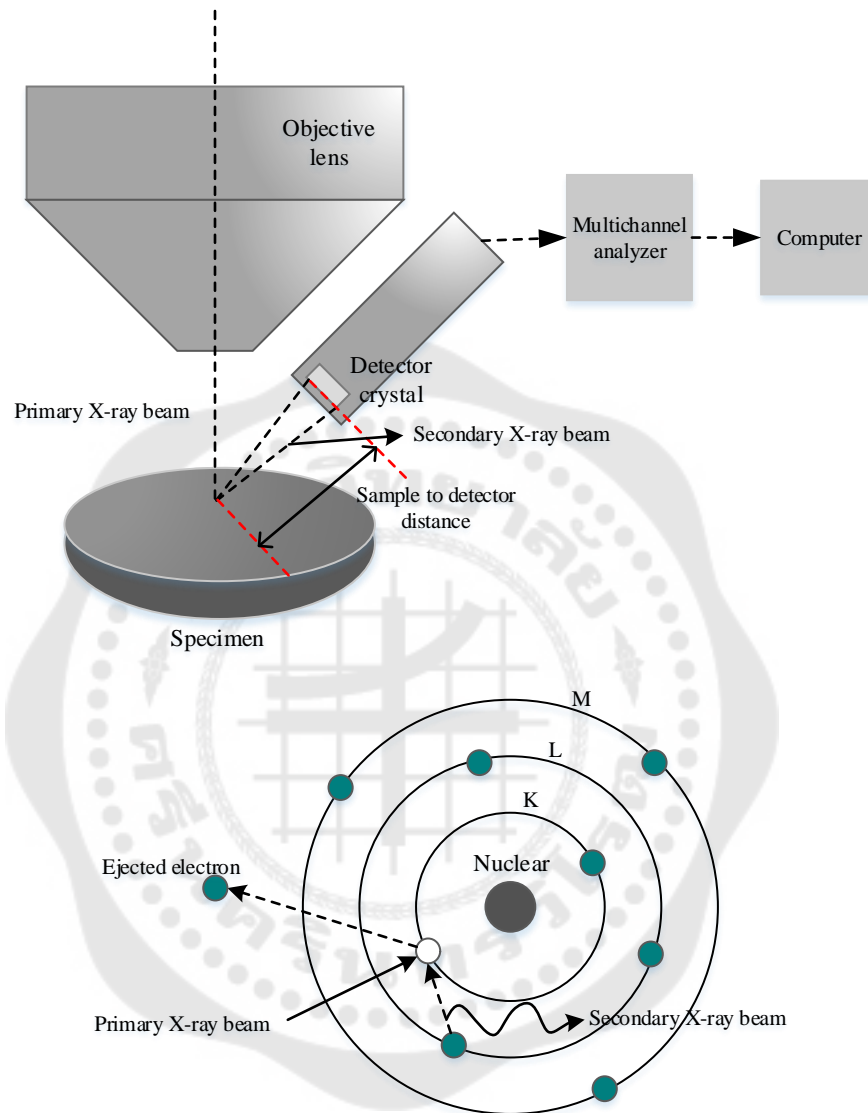


Figure 12 Energy-Dispersive X-ray Spectroscopy

Source: Goldstein, J. I., Newbury, D. E., Michael, J. R., Ritchie, N. W., Scott, J. H. J., & Joy, D. C. (2017). *Scanning electron microscopy and X-ray microanalysis*: Springer.

2.3.5 The X-ray diffraction

X-ray diffraction (XRD) is an analytical technique, which can be studied to investigate the powder or solid to describe the crystalline phase, physical properties of synthesized materials. These methods are based on observing the scattered intensity of an X-ray beam, having high energy and shorter-wavelength penetrates the surface of the synthesized sample material whose atomic planes act as a diffraction grating. X-rays are electromagnetic radiation with typical photon energies is in the range of **100 eV-100 keV**. Shorter wavelength X-rays (hard X-ray) are used for the diffraction application which is in the range of a few angstroms to **0.1 angstroms (1 keV-120 keV)**. Because the wavelength of X-rays is comparable to the size of atoms, they are ideally suited for probing the structural arrangement of atoms and molecules in a wide range of materials. The incident beam is diffracted at specific angles which represents the crystallographic structure of synthesized materials according to Bragg's law. W.L.Bragg.

$$n\lambda = 2d \sin \theta \dots\dots\dots(2.7)$$

When n is an integer representing the order of the diffraction peak.

λ is the wavelength of the X-ray

d is the lattice plane spacing

θ is the scattering angle

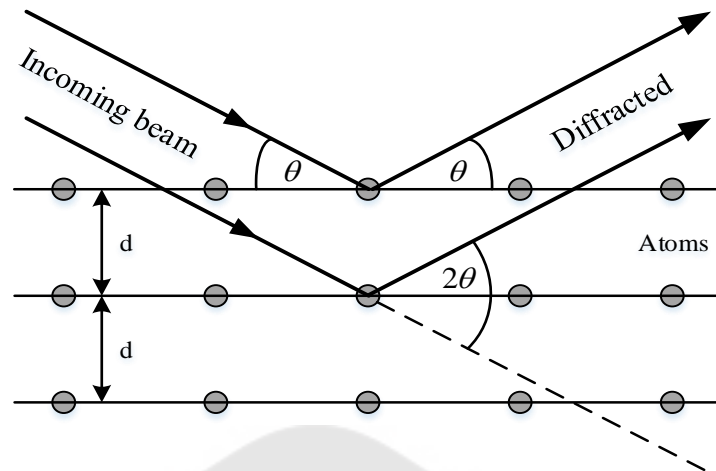


Figure 13 X-ray diffraction in crystal structure

Source: Epp, J. (2016). X-ray diffraction (XRD) techniques for materials characterization *Materials characterization using Nondestructive Evaluation (NDE) methods* (pp. 81-124): Elsevier.

CHAPTER 3

RESEARCH METHODOLOGY

In this research, we study the influence of Mn_3O_4 composition on some physical properties of Y145 superconductor prepared by solid-state reaction method. This research is related to the details of the synthesis procedure, various characterization techniques and equipment employed in the experiment. The samples of $\text{YBa}_2\text{Cu}_3\text{O}_y$, and $\text{YBa}_4\text{Cu}_5\text{O}_y$ superconductor doped with Mn_3O_4 are investigated by the study processes as following:

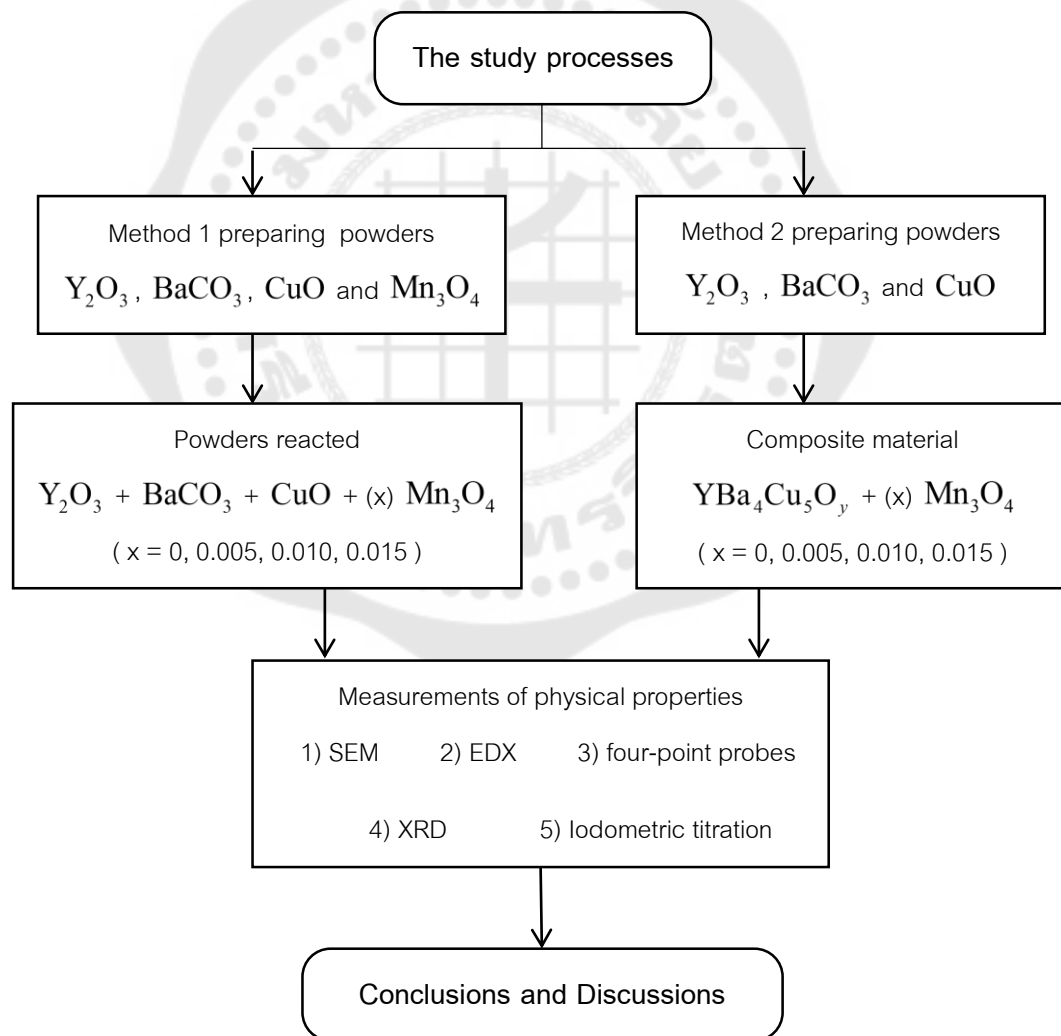


Figure 14 The procedure of research

3.1 The preparation of YBaCuO superconductors

The most popular technique for synthesizing Y123 is the standard technique of solid-state reaction. We synthesize the Y123, Y145 and Y145 doped with Mn_3O_4 superconductors. These samples are prepared by the standard solid-state reaction method, which is consistent with Udomsamuthirun et al. (2010). They synthesized the new YBaCuO superconductors by using standard solid-state reaction method as a composition of Y123 superconductor.

3.1.1 Preparing Y123 superconductor

The precursor powders used in the synthesized of Y123 superconductor consist of Yttrium Oxide (Y_2O_3), Barium Carbonate ($BaCO_3$) and Copper Oxide (CuO). These powders are calculated by the appropriate stoichiometric ratios of powders Y_2O_3 , $BaCO_3$ and CuO in the following chemical reaction.



This chemical formula reaction can be shown by the method of calculation. The calculated weight depends on the molecular weights of these oxides and carbonates with appropriate weights in proportion to their molecular weights through the chemical reaction. To determine the appropriate amounts of precursor powders, use in the synthesized of superconductors as follows:

$$\begin{aligned} \text{Molecular mass } Y_2O_3 &= \text{Atomic mass Y} + \text{Atomic mass O} \\ &= (2 \times 88.906) + (3 \times 15.999) \\ &= 225.809 \text{ u} \end{aligned}$$

Molecular mass

$$\begin{aligned} BaCO_3 &= \text{Atomic mass Ba} + \text{Atomic mass C} + \text{Atomic mass O} \\ &= 137.330 + 12.011 + (3 \times 15.999) \\ &= 197.388 \text{ u} \end{aligned}$$

$$\begin{aligned} \text{Molecular mass } CuO &= \text{Atomic mass Cu} + \text{Atomic mass O} \\ &= 63.546 + 15.999 \\ &= 79.545 \text{ u} \end{aligned}$$

All powders obtained are calculated by the chemical reaction of the molecular mass of 3 types. These have many different concentrations in the chemical reaction used. So, we can calculate the correct amounts of materials that are necessary for the preparation of Y123 superconductor as below:

$$\text{Yttrium Oxide (Y}_2\text{O}_3) : 0.5 \times 225.809 = 112.809 \text{ u}$$

$$\text{Barium Carbonate (BaCO}_3) : 2 \times 197.388 = 294.676 \text{ u}$$

$$\text{Copper Oxide (CuO)} : 3 \times 79.545 = 238.635 \text{ u}$$

In the practical, the powders are calculated by using the appropriate ratio again to avoid mistakes in the preparation. This preparation process plays an important role in understanding the powder used. Since these powders are purity and relatively high cost.

3.1.2 Preparing Y145 superconductor doped with Mn₃O₄

3.1.2.1 Calculating precursor powders of Y145 superconductor

The precursor powders are used in the synthesized of Y145 superconductor doped with Mn₃O₄. There are Yttrium Oxide (Y₂O₃), Barium Carbonate (BaCO₃), Copper Oxide (CuO), and Manganese Oxide (Mn₃O₄). These samples are synthesized by the characteristic of the compound.

The preparation process of Y145 superconductor in the chemical reaction is:



From the above chemical reaction can be shown by the method of calculation. This calculations are operated by the amount of powders in the synthesise of Y145 superconductors as:

$$\begin{aligned} \text{Molecular mass Y}_2\text{O}_3 &= \text{Atomic mass Y} + \text{Atomic mass O} \\ &= (2 \times 88.906) + (3 \times 15.999) \\ &= 225.809 \text{ u} \end{aligned}$$

Molecular mass

$$\begin{aligned} \text{BaCO}_3 &= \text{Atomic mass Ba} + \text{Atomic mass C} + \text{Atomic mass O} \\ &= 137.330 + 12.011 + (3 \times 15.999) \\ &= 197.388 \text{ u} \end{aligned}$$

$$\begin{aligned}
 \text{Molecular mass CuO} &= \text{Atomic mass Cu} + \text{Atomic mass O} \\
 &= 63.546 + 15.999 \\
 &= 79.545 \text{ u}
 \end{aligned}$$

From calculating, the appropriate stoichiometric ratios of powders Y_2O_3 , BaCO_3 , and CuO are mixed. These powders are necessary for the preparation of the Y145 superconductor. There are in following:

$$\text{Yttrium Oxide (Y}_2\text{O}_3) : 0.5 \times 225.809 = 112.809 \text{ u}$$

$$\text{Barium Carbonate (BaCO}_3) : 4 \times 197.388 = 789.340 \text{ u}$$

$$\text{Copper Oxide (CuO)} : 5 \times 79.545 = 397.725 \text{ u}$$

Besides, there is a molecular mass of Manganese Oxide (Mn_3O_4). The Mn_3O_4 is put in the chemical reaction as below:

$$\begin{aligned}
 \text{Molecular mass Mn}_3\text{O}_4 &= \text{Atomic mass Mn} + \text{Atomic mass O} \\
 &= (3 \times 54.938) + (4 \times 15.999) \\
 &= 228.810 \text{ u}
 \end{aligned}$$

3.1.2.2 Mixing Y_2O_3 , BaCO_3 , CuO and Mn_3O_4 powders reaction

The powders are prepared by the solid-state reaction method by the chemical reaction that raw materials Y_2O_3 , BaCO_3 , CuO , and Mn_3O_4 powders. These powders are mixed and ground to be the chemical homogeneity, which has different ratio concentrations according to mixed in the chemical formula as follows:

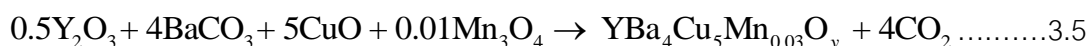
1) Formula of (Y145)



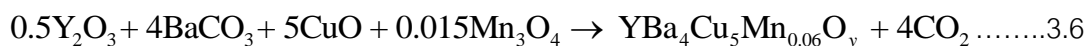
2) Formula of (Y145+0.005 Mn_3O_4)



3) Formula of (Y145+0.01 Mn_3O_4)



4) Formula of (Y145+0.015 Mn_3O_4)



A series of crystalline solid-state reacted samples of $Y_{145+x}Mn_3O_4$ where $x=0,0.005,0.010,0.015$ mole of each value of Mn_3O_4 is mixed separately. From the values of x (mole), obtained are changed to be the values of x (grams) ($x=0,0.008,0.016,0.024$ g) which each value have any different concentrations. The Y145 consists of Y_2O_3 , $BaCO_3$, CuO are also calculated by the value of grams for conveniently calculating in according to Table 1. Moreover, the amounts of $YBa_4Cu_5O_y$, $YBa_4Cu_5Mn_{0.015}O_y$ (doped with $0.005Mn_3O_4$), $YBa_4Cu_5Mn_{0.03}O_y$ (doped with $0.01Mn_3O_4$), and $YBa_4Cu_5Mn_{0.06}O_y$ (doped with $0.015Mn_3O_4$) are determined to be 8 grams.

Table 1 Calculating powders of Y145 and Mn_3O_4

Concentration of doping (mole)	Y_2O_3 (g)	$BaCO_3$ (g)	CuO (g)	Mn_3O_4 (g)
0.000	0.803	5.618	2.830	0.000
0.005	0.802	5.612	2.828	0.008
0.010	0.802	5.606	2.825	0.016
0.015	0.801	5.601	2.822	0.024

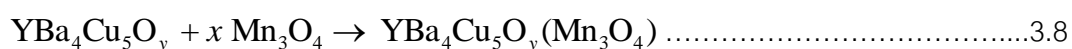
3.1.2.3 Doping Y145 with Mn_3O_4 composite material

The $YBa_4Cu_5O_y$ (Y145) powders are prepared by the solid-state reaction method by mixing the stoichiometric amount of Y_2O_3 , $BaCO_3$, CuO before doping on Mn_3O_4 according to the chemical formula reaction as follows:

1) Formula of (Y145)



2) Formula of (Y145 + xMn_3O_4)



A series of crystalline composite samples of $\text{YBa}_4\text{Cu}_5\text{O}_y + x\text{Mn}_3\text{O}_4$ where $x = 0, 0.005, 0.010, 0.015$ mole of Mn_3O_4 are mixed separately according to Table 2. The Mn_3O_4 equals to 0, 0.008, 0.016, 0.024 g are calculated. And the 8 grams of $\text{YBa}_4\text{Cu}_5\text{O}_y$ are prepared by calculating the concentration.

Table 2 Calculating Y145 superconductor doped with Mn_3O_4

Concentration of doping (mole)	Y145 (g)	Mn_3O_4 (g)
0.000	8.000	0.000
0.005	8.000	0.008
0.010	8.000	0.016
0.015	8.000	0.024

When the preparation process of powder doped with Mn_3O_4 between the solid-state reacted and the composition is finely mixed. These powders are followed by calcination two times, pressing into pellets, sintering, and annealing, respectively.

3.2 The synthesis of Y145 superconductor doped with Mn_3O_4

Synthesis means the preparation of the desired material. The selection of any material depends on the specifications required in the final product. So this work, we use the well-known solid-state reaction technique for the synthesis of modified ceramic materials, which is an important technique for synthesizing perovskite ceramic. This method gives a good quality of sample to synthesize single-phase compounds below:

1) first of all, the powders are prepared by the different concentration as Yttrium(III) oxide Y_2O_3 (99.99%, ALORICH. China), Barium carbonate BaCO_3 (99.0%, UNIVAR, India), Copper(II) oxide CuO (97%, ACROS ORGANICS, Belgium) and Manganese(II,III) oxide Mn_3O_4 (97%, ALORICH. China) showing in Figure 15. The appreciate amount of powders are weighed. These powders are mixed and ground compounds in a mortar and pestle. The hand-grinding process is almost always

essential to produce a single-phase powder to attain chemical homogeneity as Figure 16.



Figure 15 The precursor powders of the sample preparation



Figure 16 Mixed and ground powder process

2) The calcination process starts at 100 °C temperature. After this, this process is set in the increasing of temperature with a rate of 20 °C per minute according to the same curve of heat treatment, Figure 17. When the temperature reaches at 950 °C and keeps at that temperature for 24 hours, then reduced to 100 °C temperature with the rate of 2 °C per minute.

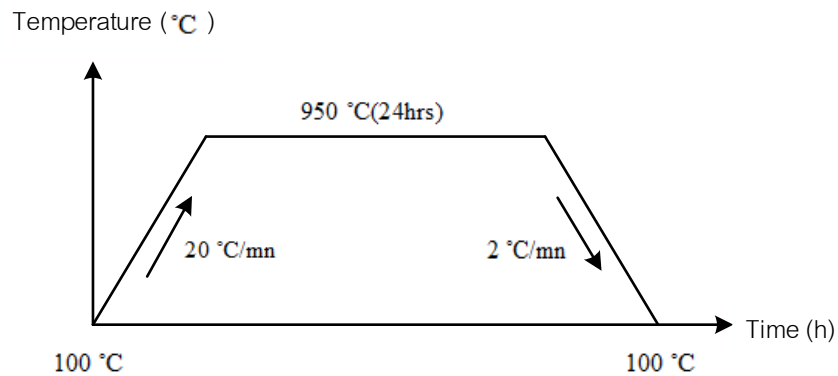


Figure 17 Calcination process for $\text{YBa}_4\text{Cu}_5\text{O}_y$

3) The mixed materials are strong black shown in Figure18. In the next process, the product obtained from calcination is reground by a fine powder in a mortar and pestle to be homogenous. Calcination is repeated twice with intermediate grains powder obtained, then this powder is poured into the alumina cup for taking it to calcine in the furnace again.



Figure 18 The calcined powders

4) The calcined powders are reground in the mortar and pestle for obtaining the fine powders mixture. The powders are compressed by the hydraulic press machine for 30 minutes. These powders are pressed into pellets with 3.0 cm in diameter and about 5.0 mm in thickness under 15000 N/m^2 pressure shown in Figure 19. The samples obtained are sintered in the next process.



Figure 19 The pellets sample of $\text{YBa}_4\text{Cu}_5\text{O}_y$

5) The sintering process starts at $100\text{ }^\circ\text{C}$ temperature. This process is set in the increasing of temperature with a rate of $20\text{ }^\circ\text{C}$ per minute according to this curve of heat, Figure 20. After that, when the temperature reaches at $950\text{ }^\circ\text{C}$ and keeps at temperature for 24 hours. Then, the temperature is decreased to $550\text{ }^\circ\text{C}$ with a rate of $2\text{ }^\circ\text{C}$ per minute. Finally, the process is an important role for the annealing process, the samples are annealed at $550\text{ }^\circ\text{C}$ for 24 hours in the air and decreased to $100\text{ }^\circ\text{C}$ temperature with a rate of $2\text{ }^\circ\text{C}$ per minute.

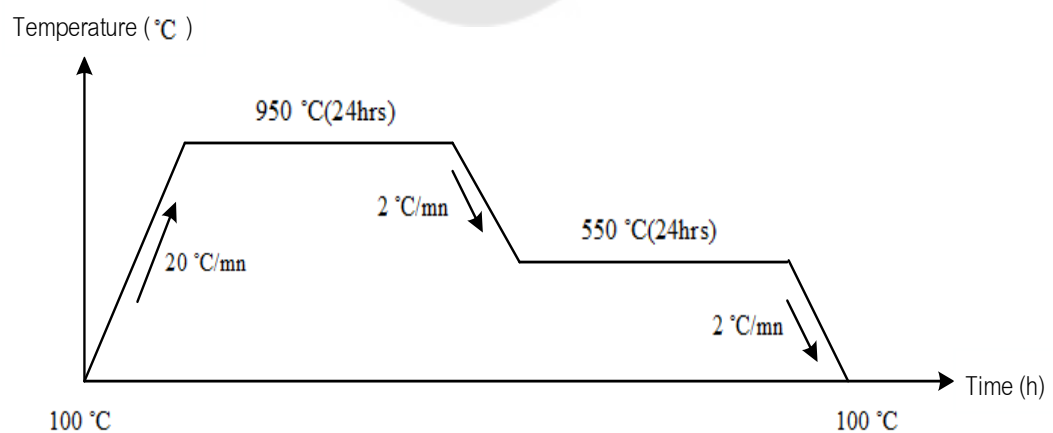


Figure 20 Sintering and annealing of $\text{YBa}_4\text{Cu}_5\text{O}_y$ doped with Mn_3O_4

In this synthesis process, which is a crucial role in synthesizing **Y145** superconductor and **Y145** superconductor doped with Mn_3O_4 by solid-state reaction showing in Figure 21. And the samples obtained are investigated by the physical properties of superconductor as SEM, EDX, four-point probes, and XRD, respectively.

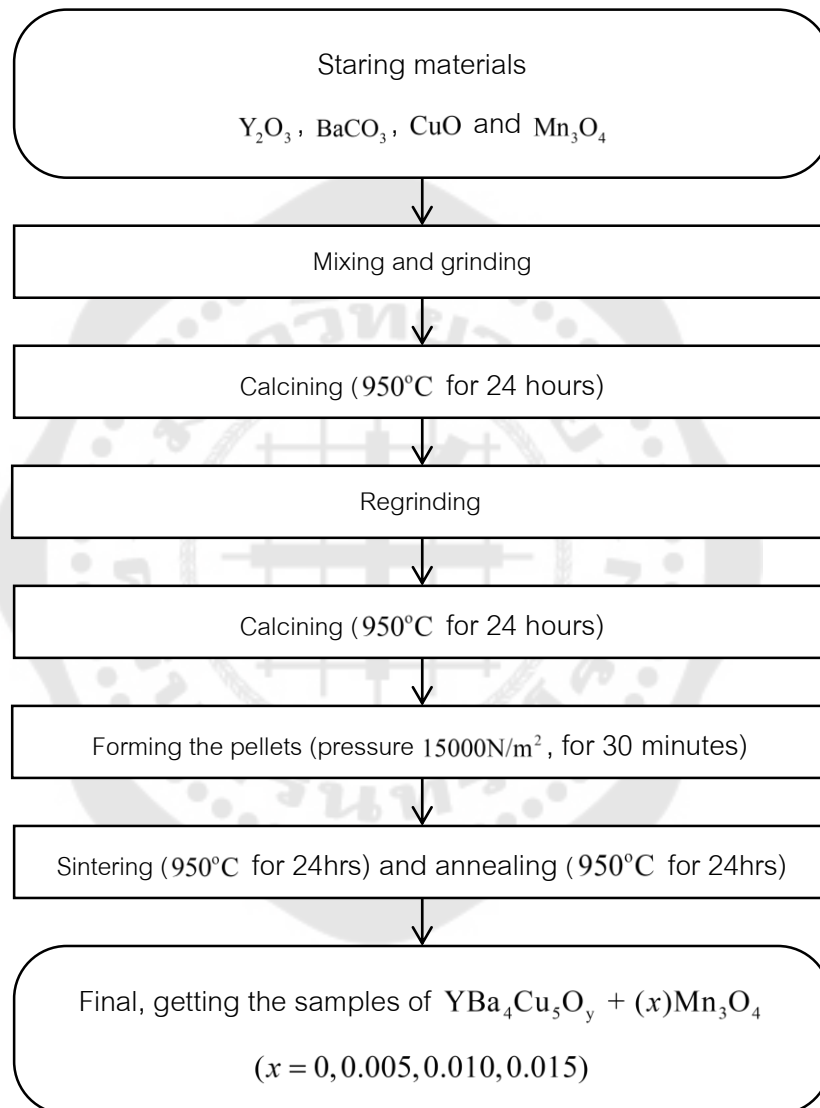


Figure 21 The synthesis procedure in the solid-state reaction technique.

3.3 Measurement procedure

3.3.1 The Electrical Resistance measurement

In this process, the physical properties are analyzed by the electrical resistance. The resistance as a function of temperature is set in a range of 77 K - 120 K by using liquid nitrogen. the electrical resistance is measured by the four-point method to find the value of the critical temperature of superconductor and the value of resistivity of superconductor. There are equipment as following:

- 1) Coaxial Cable number TSLE 156277
- 2) Thermocouple type K
- 3) Thermocouple (NI USB-TC01, Hungary)
- 4) DC power supply (HY3005D, China)
- 5) Digital precision multimeter (Fluke 8845A6-1/2, USA)
- 6) Computer

3.3.2 Making the probe and measuring the electrical resistance

1) the measurement process is measured by a standard D.C four-point probes method. The probes are created by a stainless nut which has 2 mm in diameter and 10 mm in distance probes by using the conductive epoxy (silver paint: part A and B, Cw2400) is connected. There are 4 probes, as two probes are used for connecting the current and two probes are used for connecting the voltage. Both voltage and current contacts are made with silver paint to minimize the contact resistance.

2) The equipment-set in the measurement of electrical resistance is shown in Figure 22. The experiment is used for four-point probes method by the current and voltage are attached to the superconductor and the circuit in the program. The program is set at low temperatures down to 77 K . A temperature value, where the resistance starts to increase significantly, is determined to be the onset critical temperature (T_c onset) of the sample whereas the offset transition temperature (T_c offset) is defined as the temperature at which resistance equal to zero.

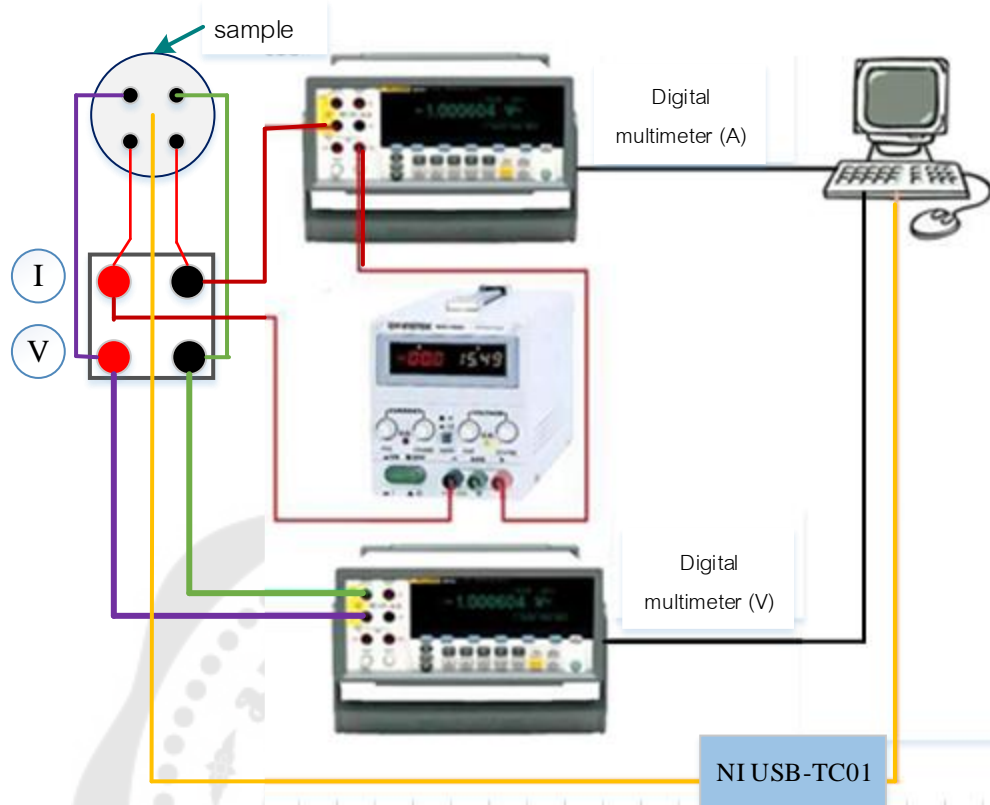


Figure 22 Equipment for measuring the electrical resistance of a superconductor

Since this material will occur the superconductivity at low temperature, which uses liquid nitrogen for being coolant and decreasing the temperature of superconductor. When the temperature of superconductor is cooled at 77 K . To start a voltage source and a constant current (current kept a constant at 200 mA) flow through the superconductor. When the temperature reach at 120 K to saving data on the computer. And then we calculate the voltage difference (V) and electric current (I) to find the electrical resistivity (ρ).

3.3.3 Measuring resistance of the van der Pauw method

The characteristic of measurement is arranged by the four-point probes method. The probes are mounted into the probe station carefully and their position is adjusted. The wires are then connected with probes and source meter. After that, the measurement process is started around the sample according to Figure 23 by having many characterizations as follows:

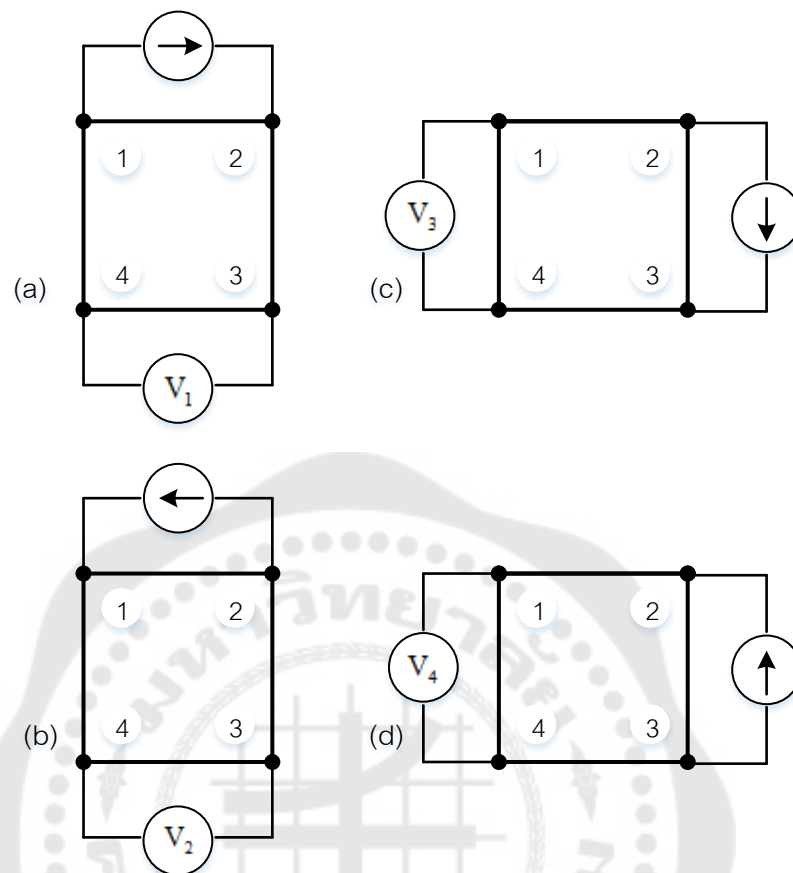


Figure 23 Van der Pauw measurement structure

In Figure 23, the four-point probe numbered 1, 2, 3, 4, which are connected to the superconductor. Probe 1 and 2 are the current probes (a). Probe 3 and 4 are the voltage probes (b). Also in this figure, notice that a constant current source (200 mA) is used. The current source is switched by moving on to all sides of the sample. Afterward, the data from measuring the four-point probes shown in the computer can be calculated by the related the two resistance ratios Q equation (2.5) and the geometrical factors f equation (2.4), respectively. And the resistivity ρ can compute from the equation (2.2).

3.4 Iodometric Titration

In this study, the characteristics of precursor powders are carried out by the iodometric titration technique. This titration is used for determining the amount of Cu^{2+} , Cu^{3+} and oxygen content. The oxygen content O_y are calculated by using the sum of

the oxygen number of all samples. The $\text{YBa}_2\text{Cu}_3\text{O}_y$ high-temperature superconductors are examples of nonstoichiometric compounds in which the oxygen content is variable. The coefficient y in the formula has a noninteger value in the range 6.5 – 7. We will determine the oxygen content indirectly through iodometric titration of copper, which is present in both the +2 and +3 oxidation states in $\text{YBa}_2\text{Cu}_3\text{O}_y$ (Daniel C. Harris, Hills, & Hewston, 1987).

In titration A, the total copper content of the sample will be determined after converting all of the Cu^{3+} to Cu^{2+} and allowing the Cu^{2+} to react with I^- to form I_3^- . The triiodide (I_3^-) produced is titrated with sodium thiosulfate ($\text{Na}_2\text{S}_2\text{O}_3$), hence the classification of this redox titration as an iodometric titration. The balanced chemical equation for the titration reaction is



1. remove the solid made by heating the powder from the crucible, and transfer it to a clean mortar using plastic forceps. Describe the appearance of the solid produced. Grind up a portion of the solid using the pestle.
2. accurately weigh out 100 to 150 mg of the powdered $\text{YBa}_2\text{Cu}_3\text{O}_y$ prepared, and transfer it to a clean beaker that can be used for the titration.
3. In a fume hood, dissolve the $\text{YBa}_2\text{Cu}_3\text{O}_y$ powder in 10mL of 1.0 M the perchloric acid solution (HClO_4).
4. Boil the mixture gently for 10 minutes. Do not allow this solution to boil to dryness. While the sample is boiling gently under the supervision of one member of your lab group, the other member can prepare the second and third titration samples following the procedures given in Steps 1-4.
5. Allow these solutions to cool to room temperature before beginning the titration.
6. Dissolve 1.0 -1.5 g of the potassium iodide (KI) in 10 mL of distilled water, and immediately add the solution to the beaker containing the dissolved $\text{YBa}_2\text{Cu}_3\text{O}_y$. Begin magnetic stirring. Do not carry out this step until you are completely set up to do the titration.

7. Titrate with the standardized sodium thiosulphate solution ($\text{Na}_2\text{S}_2\text{O}_3$) provided. Be sure to record the concentration of the standardized $\text{Na}_2\text{S}_2\text{O}_3$ and starting volume of $\text{Na}_2\text{S}_2\text{O}_3$ in the buret. Add 3 mL of starch solution just before the last trace of the I_2 to the starch, making it difficult to see the endpoint. Note: the triiodide ion I_3^- exists in equilibrium with I_2 and I^- which is the reason the solution has the orange/brown color characteristic of $\text{I}_{2(\text{aq})}$. The solution should turn blue when the starch is added.

8. Titrate slowly from this point on. The blue color will disappear at the endpoint leaving a cloudy white mixture. This solution containing suspended white solids should remain white for 30 – 60 s. If the solution turns blue, you have just observed a false endpoint and you should continue titrating slowly. Once you have reached the endpoint, record the volume of $\text{Na}_2\text{S}_2\text{O}_3$ remaining in the buret.

9. Repeat this procedure (steps 6 -8) two additional times.

In titration B, both Cu^{2+} and Cu^{3+} will be reacted with I^- each mole of Cu^{+2} producing half a mole of I_3^- and each mole of Cu^{3+} producing one mole of I_3^- . The results of these titrations will be used to determine for oxygen can then be calculated based on the distribution of copper between the two oxidations states (Daniel C Harris & Hewston, 1987).

1. remove the solid made by heating the powder from the crucible, and transfer it to a clean mortar using plastic forceps. Describe the appearance of the solid produced. Grind up a portion of the solid using the pestle.

2. accurately weigh out 100 to 150 mg of the powdered $\text{YBa}_2\text{Cu}_3\text{O}_y$ prepared, and transfer it to a clean beaker that can be used for the titration.

3. In a fume hood, add the potassium iodide (KI) 15 mL of 10% of the powdered $\text{YBa}_2\text{Cu}_3\text{O}_y$ prepared, and place it in an Erlenmeyer flask.

4. Remove dissolved oxygen from the solution by vigorously bubbling nitrogen through the solution for 10 minutes. Nitrogen can be delivered to the solution by attaching a Pasteur pipette to the end of nitrogen line. Make sure that the tip of the Pasteur pipette remains submerged.

5. Add 6 mL of 3.5 M HCl solution to the Erlenmeyer flask over a 5-minute period, while stirring the solution magnetically. We should gently bubble nitrogen through the solution as you complete the remainder of the titration procedure. The solution should turn brown as the HCl is added indicating the formation of triiodide.

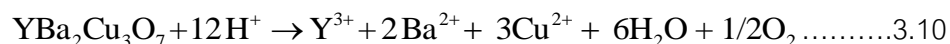
6. Continue to stir the solution for 10 minutes after the addition of the HCl solution is complete. We will eventually see formation of a grayish white precipitate when the concentration of CuI in the reaction mixture exceeds its solubility.

7. Titrate with the standardized solution of Na₂S₂O₃ provided. Be sure to record the concentration of the standardized Na₂S₂O₃ and starting volume of Na₂S₂O₃ in the buret. Add 3 mL of starch solution just before the last trace of the I₂ to the starch, making it difficult to see the endpoint. Note: the triiodide ion I₃⁻ exists in equilibrium with I₂ and I⁻ which is the reason the solution has the orange/brown color characteristic of I_{2(aq)}. The solution should turn blue when the starch is added.

8. Titrate slowly from this point on. The blue color will disappear at the endpoint leaving a cloudy white mixture. This solution containing suspended white solids should remain white for 30 – 60 s. If the solution turns blue, you have just observed a false endpoint and you should continue titrating slowly. One you have reached the endpoint, record the volume of Na₂S₂O₃ remaining in the buret.

9. Repeat this procedure (steps 6 -8) two additional times.

Titration A: As described above, the copper present in the 1-2-3 high-temperature superconductors exists in the +2 and +3 oxidation states. The titration determines the total amount of copper present in the sample. All of the Cu³⁺ present in the samples is converted to Cu²⁺ through oxidation-reduction reaction with the strong acid (HClO₄)(Choy et al., 1988)



Iodide I⁻ is added to the sample and reacts with Cu²⁺ to produce triiodide I₃⁻, the species titrated with Na₂S₂O₃.



Equation 1 shows the reaction between I_3^- and $\text{S}_2\text{O}_3^{2-}$ which occurs in the titration. Determine the number of moles of I_3^- titrated, which is related to the copper content as follows

$$2n_A(\text{I}_3^-) = n_A(\text{Cu}_{\text{total}}) = [n_A(\text{Cu}^{2+}) + n_A(\text{Cu}^{3+})] \dots\dots\dots 3.12$$

Where the quantities $n_A(y)$ represent the number of moles of species y present in sample A or required to titrate sample A. To find the number of moles of each species present in a l-g sample or required to titrate a l-g sample, divide equation 3.12 by the mass of sample A, m_A .

$$2n_A(\text{I}_3^-) / m_A = n_A(\text{Cu}_{\text{total}}) / m_A = [n_A(\text{Cu}^{2+}) + n_A(\text{Cu}^{3+})] / m_A \dots\dots\dots 3.13$$

$$2n_A(\text{I}_3^-) / m_A = n(\text{Cu}_{\text{total}}) = [n(\text{Cu}^{2+}) + n(\text{Cu}^{3+})] \dots\dots\dots 3.14$$

Where $n(y)$ represents the number of moles of species y in a l-g sample. Division of equation 3.12 by the mass of the sample makes the number of moles independent of sample size and permits comparison of the results from titrating samples of differing sizes. Find the quantity $2n_A(\text{I}_3^-) / m_A$ for each titration. Report the average and standard deviation of $2n_A(\text{I}_3^-) / m_A$ for the three titrations.

Titration B: in this titration, any copper present in the +3 oxidation state is left in this oxidation state and is allowed to react with iodide.



The reaction of Cu^{2+} is given above in equation 3.11. Note the difference in the yield of I_3^- for the two different reactions. One mole of I_3^- is produced for every mole of Cu^{3+} in the sample, while only one half mole of I_3^- determined in the titration and the moles of Cu^{2+} and Cu^{3+} is

$$n_B(\text{I}_3^-) = 1/2n_B(\text{Cu}^{2+}) + n_B(\text{Cu}^{3+}) \dots\dots\dots 3.16$$

Divide equation 3.16 by m_B , the mass of $\text{YBa}_2\text{Cu}_3\text{O}_y$ used in each titration, to get an expression that relates the quantity of I_3^- titrated to the moles of Cu^{2+} and Cu^{3+} in a l-g sample of $\text{YBa}_2\text{Cu}_3\text{O}_y$.

$$n_B(\text{I}_3^-) / m_B = 1/2n(\text{Cu}^{2+}) + n(\text{Cu}^{3+}) \dots\dots\dots 3.17$$

Find the quantity $n_B(\text{I}_3^-)/m_B$ for each titration. Report its average and standard deviation from the three titrations.

Analysis: equations 3.14 and 3.17 can be solved simultaneously to determine the number of moles of Cu^{2+} and Cu^{3+} in a 1-g sample of $\text{YBa}_2\text{Cu}_3\text{O}_y$. To determine the moles of Cu^{2+} in a 1-g sample of $\text{YBa}_2\text{Cu}_3\text{O}_y$, subtract equation 3.17 from equation 3.14 and solve for $n(\text{Cu}^{2+})$, which yields the expression.

$$n(\text{Cu}^{2+}) = 2 \left[2n_A(\text{I}_3^-) / m_A - n_B(\text{I}_3^-) / m_B \right] \dots\dots\dots 3.18$$

Substitution of the resulting value for $n(\text{Cu}^{2+})$ into equation 3.14 and 3.17 will permit determination of $n(\text{Cu}^{3+})$. Using the value for $n(\text{Cu}^{2+})$ and $n(\text{Cu}^{3+})$, calculate the percentage of copper atoms that are in the +2 and +3 oxidation states. With this information, we could rewrite the formula for the high-temperature superconductor as $\text{YBa}_2\text{Cu}_{3(0.xx)}^{\text{II}}\text{Cu}_{3(0.zz)}^{\text{III}}\text{O}_y$, where (0.xx) and (0.zz) represent the percentages of Cu^{2+} and Cu^{3+} , respectively. Use the normal oxidation states for barium and oxygen and an oxidation state of +3 for yttrium to determine the stoichiometric coefficient y for oxygen.

Where $n(\text{Cu}^{2+})$ is number of moles of Cu^{2+}

$n(\text{Cu}^{3+})$ is number of moles of Cu^{3+}

$n_A(\text{I}_3^-)$ is number of moles of I_3^- titrated with $\text{Na}_2\text{S}_2\text{O}_3$ in titration A

$n_B(\text{I}_3^-)$ is number of moles of I_3^- titrated with $\text{Na}_2\text{S}_2\text{O}_3$ in titration B

m_A is the mass of superconductors in titration A

m_B is the mass of superconductors in titration B

We can calculate to find the amount of Cu^{2+} and Cu^{3+} following the equation 3.18 and 3.17, respectively.

Table 3 The titration results of Y123 superconductor

trial	Titration A				Titration B			
	1	2	3	Aver.	1	2	3	Aver.
Y123 sample (mg)	158.00	162.00	151.00	157.00	149.00	151.00	156.00	152.00
Na ₂ S ₂ O ₃ used (cm ³)	23.30	23.90	22.30	23.17	27.00	27.80	27.70	27.83

Number of moles of I₃⁻ is substituted by number of moles of Na₂S₂O₃

Molarity of Na₂S₂O₃ equal to 0.0379 M

Number of moles of Na₂S₂O₃ in titration A = (0.0379 × 23.17) ÷ 1000 =
0.000878

Number of moles of Na₂S₂O₃ in titration B = (0.0379 × 27.83) ÷ 1000 =
0.001054

Calculations Cu²⁺

From equation 10 to substitute, we get

$$\begin{aligned} n(\text{Cu}^{2+}) &= 2 \left[2n_A(\text{I}_3^-) / m_A - n_B(\text{I}_3^-) / m_B \right] \\ &= 2 \left[(2 \times 0.000878) / 157 - (0.001054) / 157 \right] \\ &= 8.494 \times 10^{-6} \end{aligned}$$

Calculations Cu³⁺

From equation 9 to substitute, we get

$$n_B(\text{I}_3^-) / m_B = 1 / 2n(\text{Cu}^{2+}) + n(\text{Cu}^{3+})$$

$$\begin{aligned} n(\text{Cu}^{3+}) &= n_B(\text{I}_3^-) / m_B - 1 / 2n(\text{Cu}^{2+}) \\ &= (0.001054) / 157 - 1 / 2(8.494 \times 10^{-6}) \\ &= 2.692 \times 10^{-6} \end{aligned}$$

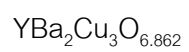
The mole ratio of Cu²⁺ : Cu³⁺ = 1 : 0.317

So, the sum of the oxidation numbers of YBa₂Cu₃O_y

$$(+3) + 2(+2) + 3 \left[\left(\frac{1}{1+0.317} \right) \times (+2) + \left(\frac{0.317}{1+0.317} \right) \times (+3) \right] + y(-2) = 0$$

$$y = 6.862$$

So that, we find that the $\text{YBa}_2\text{Cu}_3\text{O}_y$ has the chemical formula of



CHAPTER 4

RESEARCH RESULTS

The research carried out in chapter 3 is to prepare the Y145 superconductors doped with different concentrations manganese oxides ($x = 0, 0.005, 0.010, 0.015$) and to measure the physical properties of the Y145 superconductors by SEM, EDX, four-point probes, XRD and iodometric titration, respectively. In this chapter, we would like to obtain the analysis of the result from the experimental data which has the following details.

4.1 Resistivity measurements

The critical temperature of samples of Y145 superconductors were investigated by aid of D.C four-point probes technique which has 2 mm in diameter and 10 mm in distance probes by using liquid nitrogen. When the temperature of superconductor is cooled at 77 K. We will start a voltage source and a constant current at 200 mA flow through the superconductor. The physical properties are analyzed by the electrical resistance as a function of the temperature in a range of 77 K – 120 K. After that, we take the measured values from data to calculate the value of resistivity (ρ) at 120 K to plot graphs a relationship between the resistivity and the temperature. And then we find the value of the critical temperature of superconductors by using Murase method. These results are illustrated below.

4.1.1 Critical temperature of powders reacted

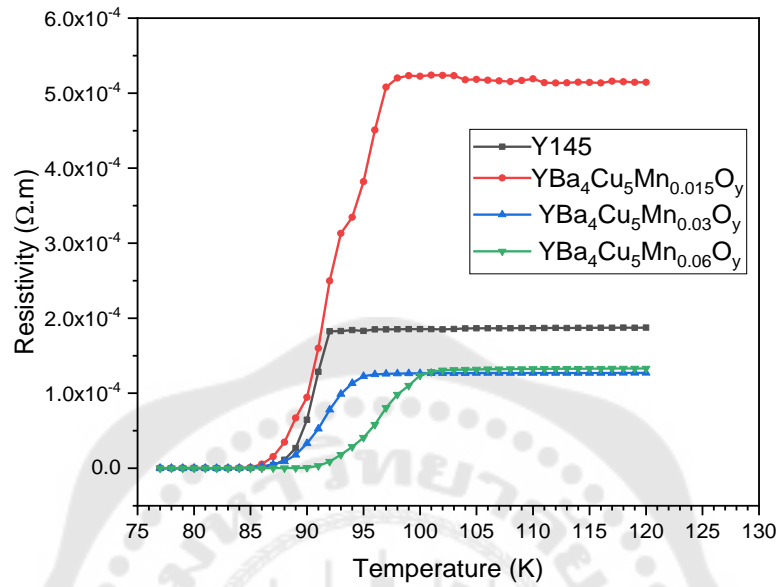


Figure 24 Resistivity dependence on the temperature for all powder reacted samples

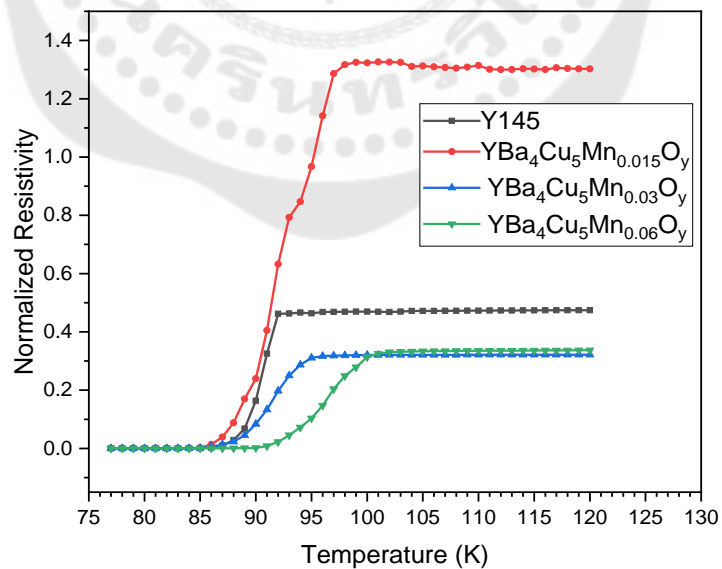


Figure 25 Show the normalized resistivity and the temperature of all powder reacted samples

Table 4 Variation of normal state and superconducting parameter in different doped samples

Samples	T_{offset} (K)	T_{onset} (K)	ΔT (K)	ρ (m Ω .cm)
Y145	89	92	3	39.5
YBa ₄ Cu ₅ Mn _{0.015} O _y	88	97	9	20.5
YBa ₄ Cu ₅ Mn _{0.03} O _y	88	95	7	32.2
YBa ₄ Cu ₅ Mn _{0.06} O _y	92	101	9	43.3

The resistivity measurement depending on temperature all samples obtained is conducted with four-point probe technique in rang 77 - 120 K. The critical temperature of Y145 superconductors are already shown in Figure 24, 25. In specially, the Y145 superconductors are synthesized by powders reacted process and investigated the influence of Mn₃O₄ by the critical temperature of all samples in the variation of normal state and superconducting parameter in different doped samples of T_c onset and T_c offset shown in Table 4.

The highest critical temperature is in YBa₄Cu₅Mn_{0.06}O_y powder reacted sample with T_c onset at 101 K and the lowest is found in pure Y145 at 92 K. For YBa₄Cu₅Mn_{0.015}O_y sample is the T_c onset at 97 K and T_c offset at 88 K. The sample of YBa₄Cu₅Mn_{0.03}O_y at T_c onset 95 K and T_c offset 88 K. The critical temperature onset and offset are readed out from these data that are represented in Table 4. These results are consistent with Chainok et.al. found that the critical temperature onset of Y145 superconductors at 94 K and 96 K prepared by solid-state reaction and melt process. According to Salama et.al reported that the critical temperature onset of Y123 superconductor doping on Mn₃O₄ with magnetic nano metal oxides at 119 K prepared by solid-state reaction. In addition, the doping on Mn₃O₄ into the Y145 superconductors by powders reacted are increased significantly in the higher critical temperature.

4.1.2 Critical temperature of composite material

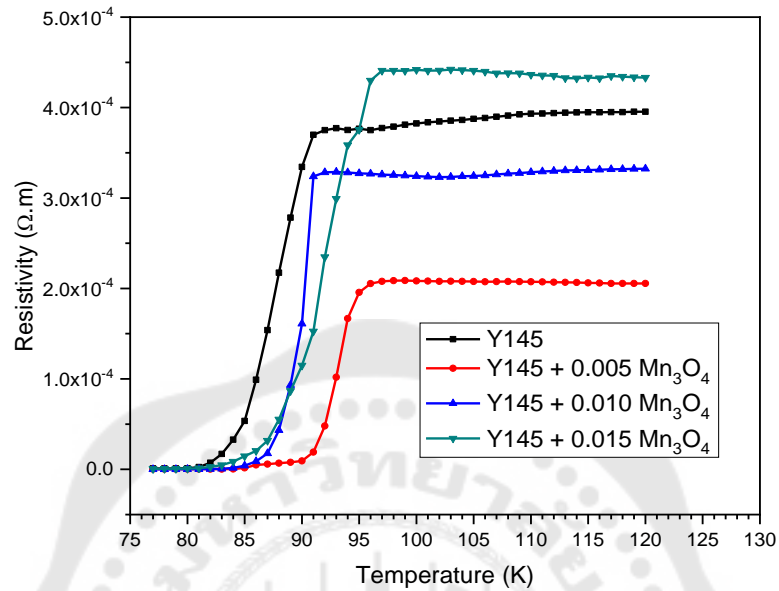


Figure 26 Resistivity dependence on the temperature for all composite material samples

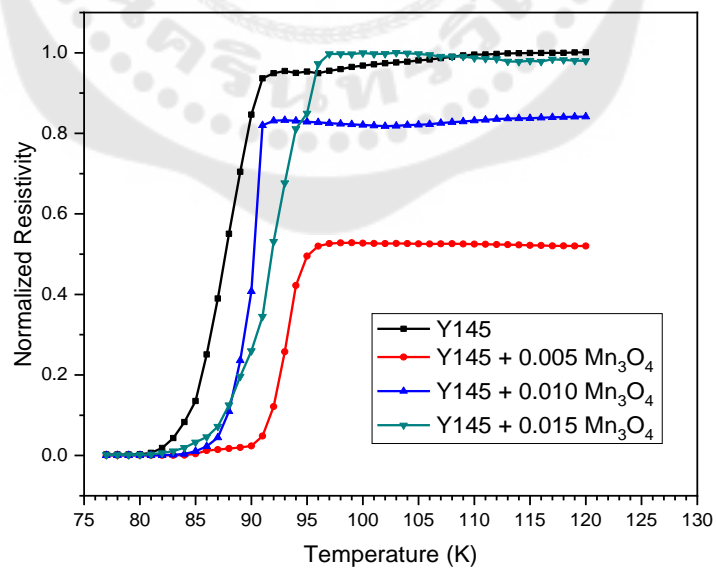


Figure 27 Show the normalized resistivity and the temperature of all composite material samples

Table 5 Variation of normal state and superconducting parameter in different doped samples

Samples	T_{offset} (K)	T_{onset} (K)	ΔT (K)	ρ ($\text{m}\Omega \cdot \text{cm}$)
Y145	84	91	7	18.7
Y145 + 0.005 Mn_3O_4	91	95	4	51.5
Y145 + 0.010 Mn_3O_4	88	92	4	12.7
Y145 + 0.015 Mn_3O_4	88	97	9	13.3

The critical temperature of all samples of Y145 doping on Mn_3O_4 superconductors in the composite materials are investigated by aid of the D.C electrical resistivity measurement using a constant current of 200 mA and the temperature is measured by thermocouple type K. The results are illustrated in Figure 26, 27. In particular, the Y145 superconductors are synthesized by the composite materials process in the influence of Mn_3O_4 on critical temperature of all samples in the variation of normal state and superconducting parameter in different doped samples of T_c onset and T_c offset presented in Table 5.

The highest critical temperature is in Y145 + 0.015 Mn_3O_4 composite material sample with T_c onset at 97 K and the lowest is found in pure Y145 at 91 K. In following the Table 5. We find that the critical temperature of Y145 + 0.005 Mn_3O_4 sample is in T_c onset at 95 K and offset at 91 K. For Y145 + 0.010 Mn_3O_4 sample decreased T_c with increasing concentration in T_c onset at 92 K and offset 88 K. These results are consistent with the research of Salama et.al. found that the T_c onset at 119 K. So that, the doping on Mn_3O_4 is essentially increased T_c .

4.1.3 Critical temperature of all samples

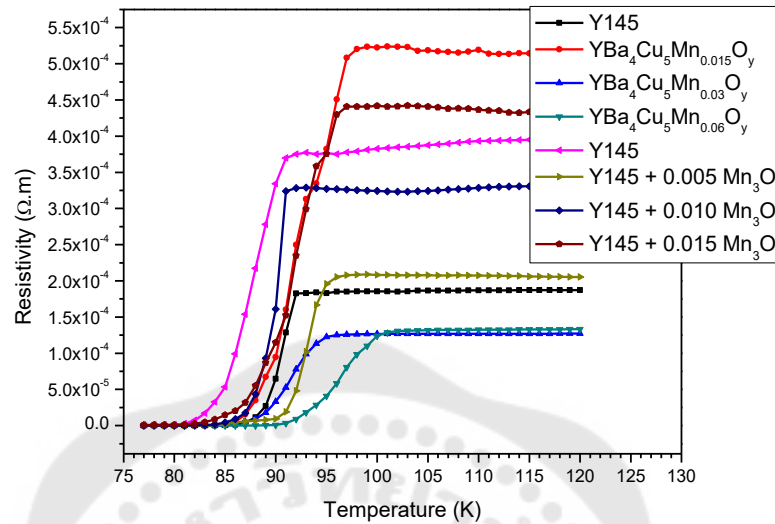


Figure 28 Comparison between the powders reacted and the composite materials samples

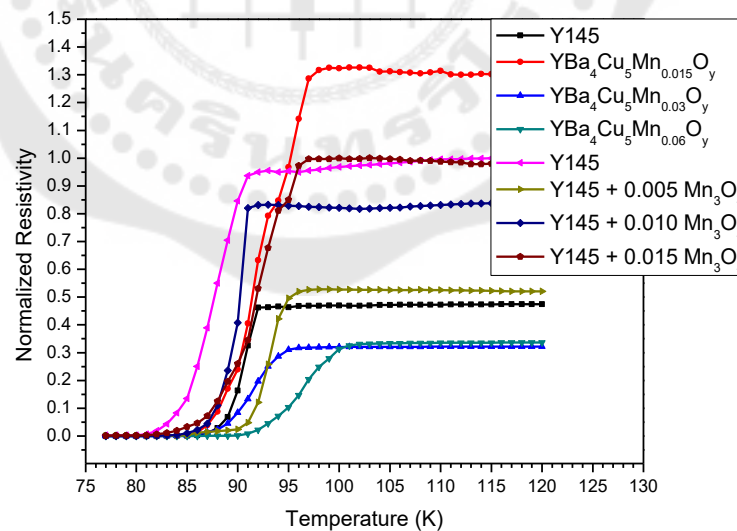


Figure 29 Shows the normalized of the powders reacted and the composite materials samples

Table 6 Variation of normal state and superconducting parameter in different samples

Samples	T_{offset} (K)	T_{onset} (K)	ΔT (K)	ρ (m Ω .cm)
Y145	89	92	3	39.5
YBa ₄ Cu ₅ Mn _{0.015} O _y	88	97	9	20.5
YBa ₄ Cu ₅ Mn _{0.03} O _y	88	95	7	32.2
YBa ₄ Cu ₅ Mn _{0.06} O _y	92	101	9	43.3
Y145	84	91	7	18.7
Y145 + 0.005 Mn ₃ O ₄	91	95	4	51.5
Y145 + 0.010 Mn ₃ O ₄	88	92	4	12.7
Y145 + 0.015 Mn ₃ O ₄	88	97	9	13.3

We have two preparation processes; the powders reacted process and the composite materials process, with different concentrations of Mn₃O₄ by the solid-state reaction. The D.C four-point probe with a constant current of 200 mA is used for a resistivity measurement with a temperature in a range of 77 to 120 K. Figure 28, 29. show the relation between the resistivity with temperature and show the normalized resistivity versus temperature of both processes that are demonstrated the critical temperature of all samples in Table 6.

According to Table 6, we also find that the two processes with different concentrations can enhance the critical temperature that the highest critical temperature onset at 101 K for YBa₄Cu₅Mn_{0.06}O_y and 97 K for Y145 + 0.015Mn₃O₄ samples, respectively. These results of magnetic micro metal oxides doping on structure and electrical properties of Y145 superconductors are consistent with the research of Salama et.al studied that the influence of magnetic nano metal oxides, in the doped with Mn₃O₄ increasing T_c significantly.

In Figure 28, the comparison of two processes on the critical temperature are shown. So that, we conclude that the critical temperature dependence of resistivity for Y145 doped samples with different concentrations of Mn₃O₄. Generally, all samples

show metallic behavior in the normal state and superconducting parameter. It is also known that the powders reacted process were higher critical temperature than the composite materials process. And then, it also shows that the doping Y145 with different concentrations of Mn_3O_4 improves the value of T_c onset at 101 K and 97 K at high doping ratios in two processes and decreases T_c with decreasing concentrations (0.010 Mole) and finally, slightly improves at 0.005 Mole to become 97 K and 95 K, respectively.

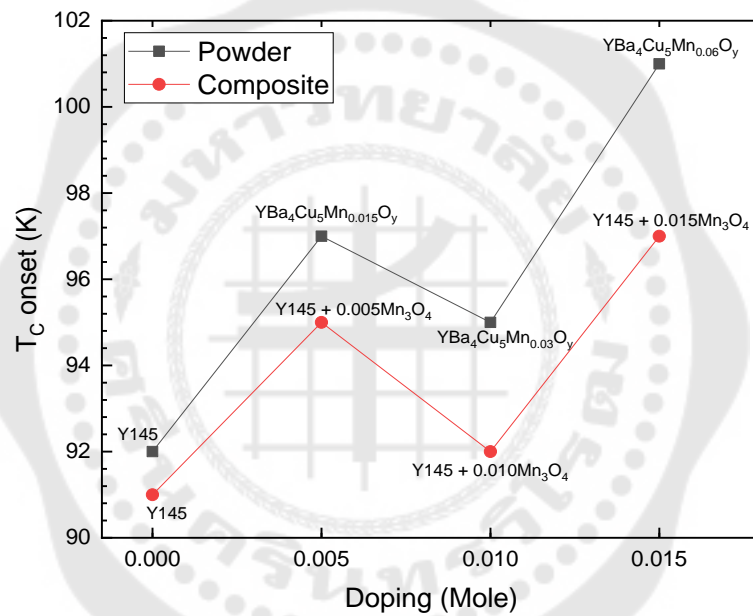


Figure 30 The concentrations versus the critical temperature onset

Table 7 This is the variation of doping and the critical temperature onset of samples.

Samples	T_{onset} (K)	Doping (Mole)
Y145	92	-
$\text{YBa}_4\text{Cu}_5\text{Mn}_{0.015}\text{O}_y$	97	0.005
$\text{YBa}_4\text{Cu}_5\text{Mn}_{0.03}\text{O}_y$	95	0.010
$\text{YBa}_4\text{Cu}_5\text{Mn}_{0.06}\text{O}_y$	101	0.015
Y145	91	-
Y145 + 0.005 Mn_3O_4	95	0.005
Y145 + 0.010 Mn_3O_4	92	0.010
Y145 + 0.015 Mn_3O_4	97	0.015

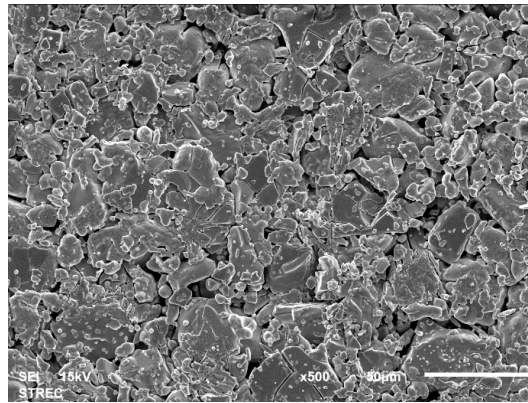
The effect of two processes and concentrations on the critical temperature onset are demonstrated. The $\text{YBa}_4\text{Cu}_5\text{Mn}_{0.06}\text{O}_y$ has the highest critical temperature onset at 101K in the powders reacted process and the $\text{Y145} + 0.015\text{Mn}_3\text{O}_4$ has the highest critical temperature onset at 97 K in the composite materials process as seen from Figure 30. The both represent that the increasing of concentrations illustrate the effect on critical temperature indirectly that increase the oxygen content and the $\text{Cu}^{3+}/\text{Cu}^{2+}$ ratio of all samples. For Mn_3O_4 doping in Table 7, we can note that there is the increase in transition temperature up to 0.015 Mole, which may be due to the Mn inclusion, which reduces the formation of other phases and enhances the formation of Y145. However, the decrease in T_c with Mn content at 0.010 Mole indicates that Mn ions have been incorporated into the Y145 structure, which results in some changes of microstructure and chemical properties of CuO_2 planes. Moreover, the possible Copper-pair breaking effect of magnetic ions is known to depress the transition temperature through the short range exchange scattering.

4.2 Scanning Electron Microscopic (SEM)

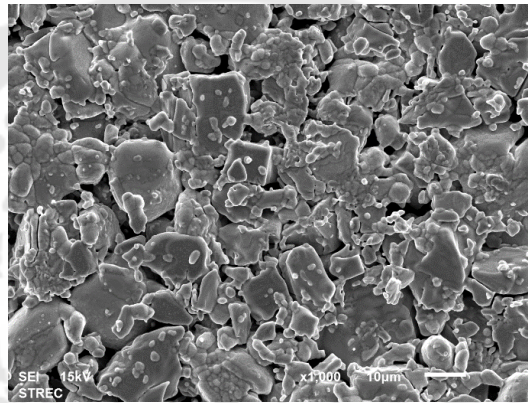
4.2.1 SEM of powders reacted

The surfaces of the samples are studied by scanning electron microscopic (SEM) in using JEOL (JSM-6610LV) as shown in Figure 31, 32, 33 and 34. For the powders reacted samples, the surfaces of $\text{YBa}_4\text{Cu}_5\text{Mn}_{0.015}\text{O}_y$, $\text{YBa}_4\text{Cu}_5\text{Mn}_{0.03}\text{O}_y$ and $\text{YBa}_4\text{Cu}_5\text{Mn}_{0.06}\text{O}_y$ are illustrated inhomogeneous as comparing to the SEM micrograph of pure Y145. The grain size of all powders reacted samples are larger grain size and more disorder than Y145. However, the doping on Mn_3O_4 of Y145 samples are less porosity than no doped.





a)

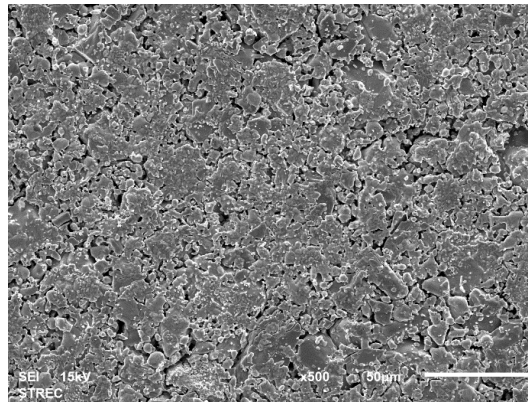


b)

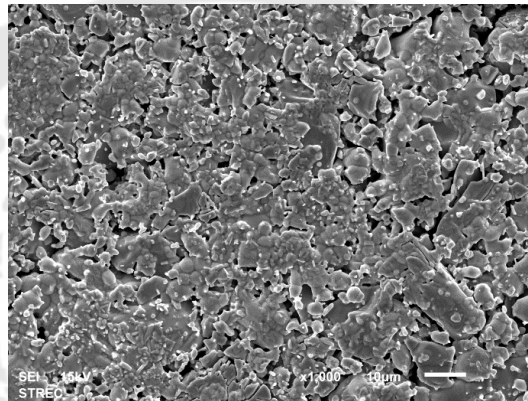


c)

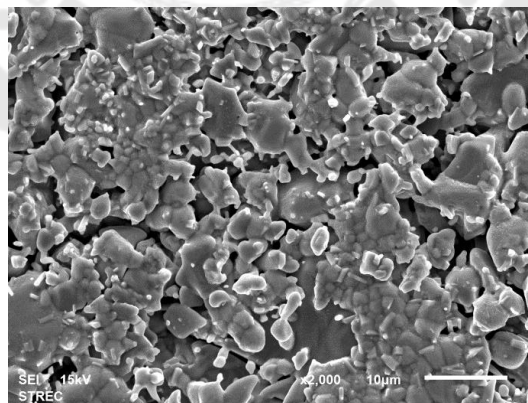
Figure 31 SEM photographs of YBa₄Cu₅O_y at the power magnifications a) 500, b) 1000 and c) 2000



a)

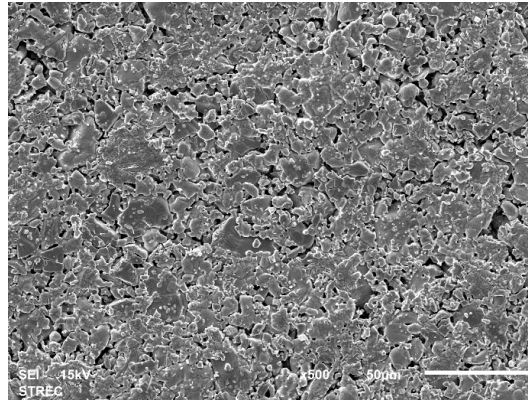


b)

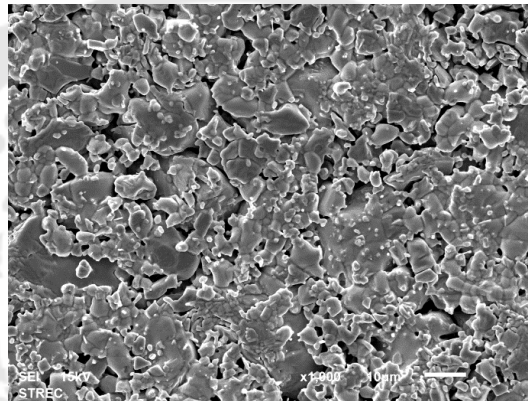


c)

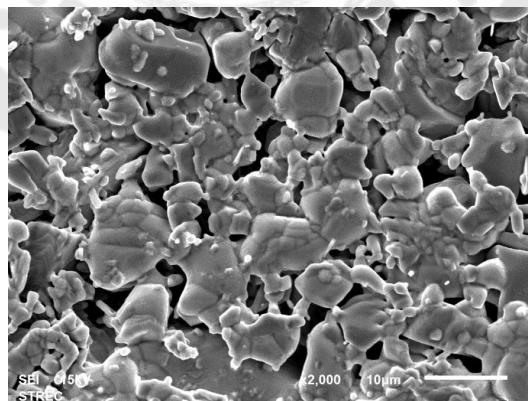
Figure 32 SEM photographs of $\text{YBa}_4\text{Cu}_5\text{Mn}_{0.015}\text{O}_y$ at the power magnifications a) 500, b) 1000 and c) 2000



a)

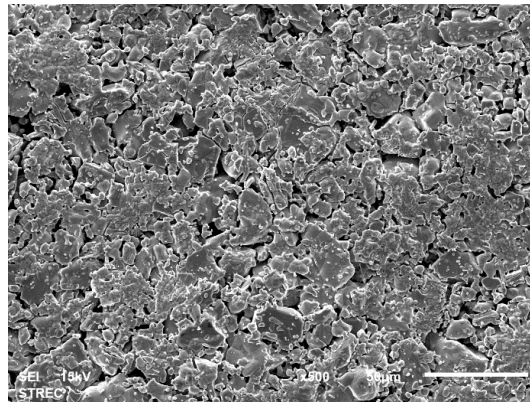


b)

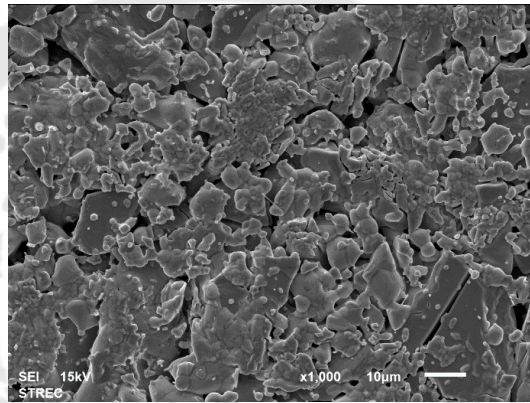


c)

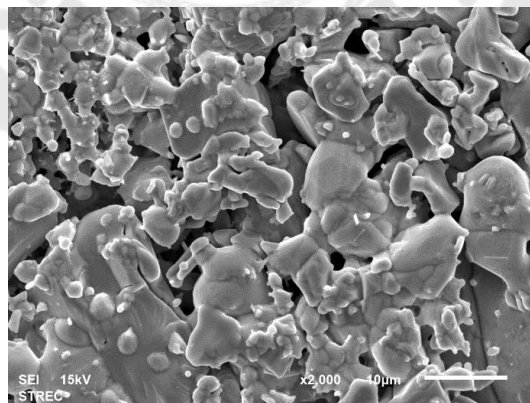
Figure 33 SEM photographs of YBa₄Cu₅Mn_{0.03}O_y at the power magnifications a) 500, b) 1000 and c) 2000



a)



b)



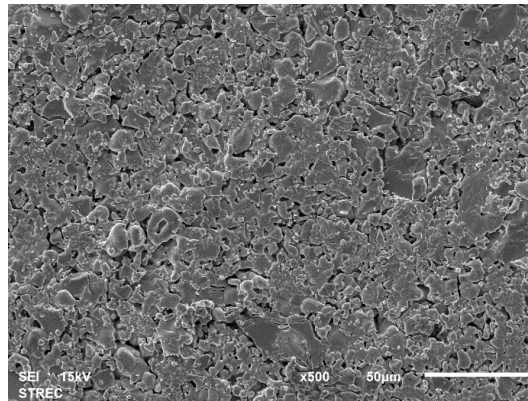
c)

Figure 34 SEM photographs of $\text{YBa}_4\text{Cu}_5\text{Mn}_{0.06}\text{O}_y$ at the power magnifications a) 500, b) 1000 and c) 2000

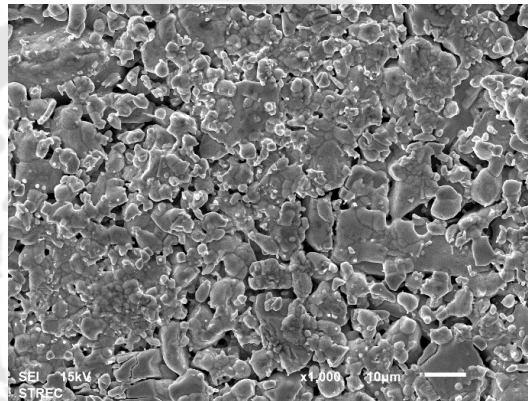
4.2.2 SEM of composite materials

This experiment, used the power magnification of 500, 1000 and 2000 for analyzing a surface of all samples according to figure 35, 36, 37 and 38 are found that the average grain size in all samples mostly does not change in most samples. The grain size of all samples exhibits large grains randomly oriented in all direction with the presence of slightly pores between the grains. For each doping on manganese oxides, it is shown that manganese oxides are not distributed randomly over the Y145 grains mostly. From figures, it is obvious that the grains of all samples are in the same range of Y145 which results of surface characteristic is consistent with research of doping on magnetic nano metal oxides (Salama et al, 2016) found that the particularly Y123 superconductor doped with Mn_3O_4 that nanodots are distributed randomly over the Y123 grains and all samples are in the same range 1-4 μm .

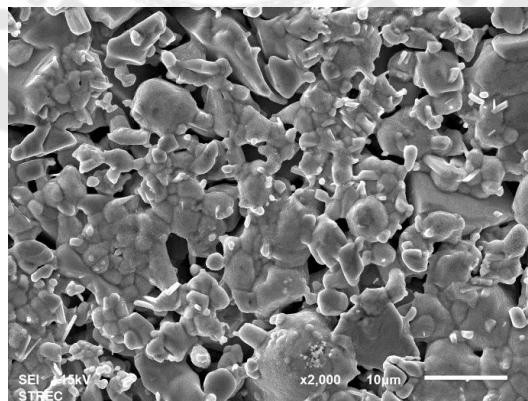
The scanning electron microscopic (SEM) images of Y145 doped with 0.005, 0.010 and 0.015 Mn_3O_4 samples are presented in figures 35, 36, 37 and 38, respectively.



a)



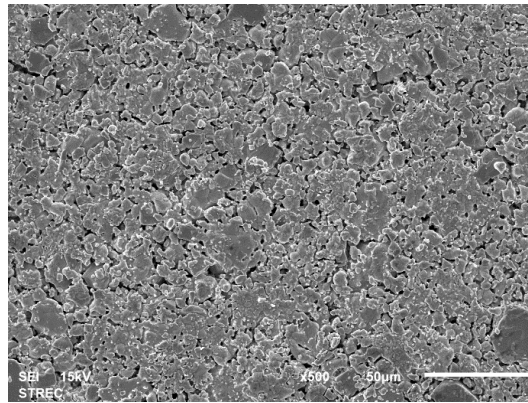
b)



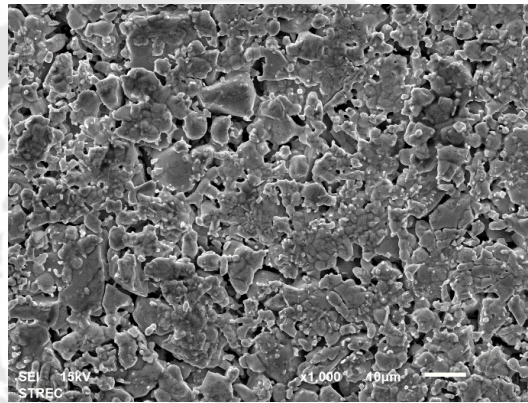
c)

Figure 35 SEM photographs of Y145 at the power magnifications a) 500, b) 1000 and c)

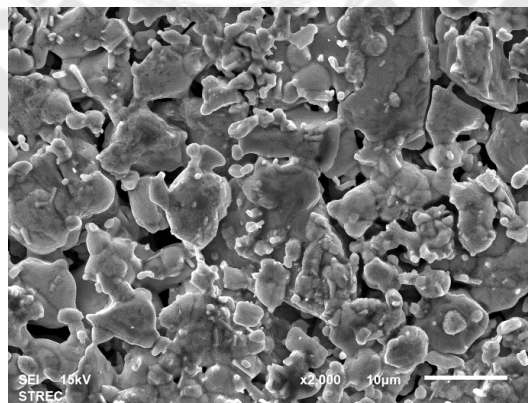
2000



a)

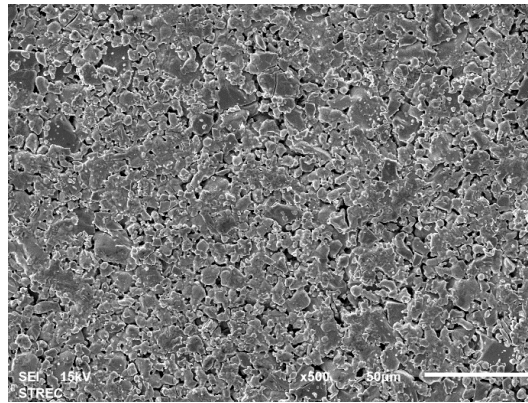


b)

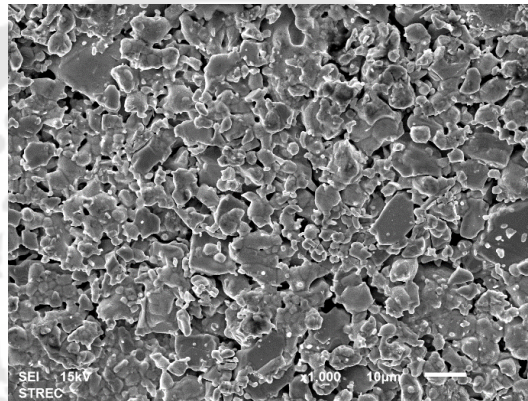


c)

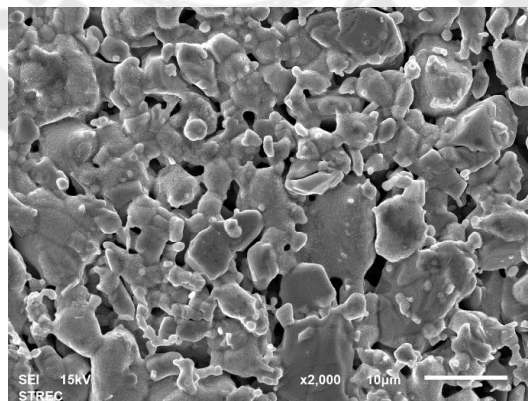
Figure 36 SEM photographs of Y145 + 0.005 Mn₃O₄ at the power magnifications a) 500, b) 1000 and c) 2000



a)

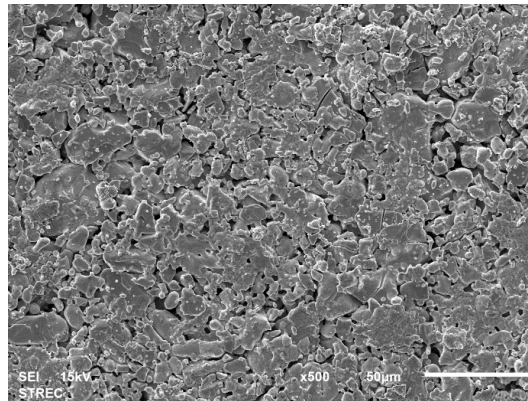


b)

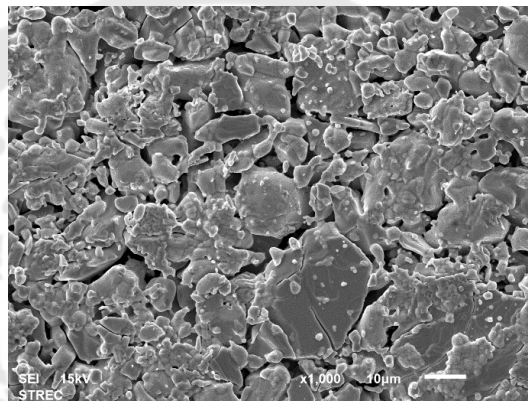


c)

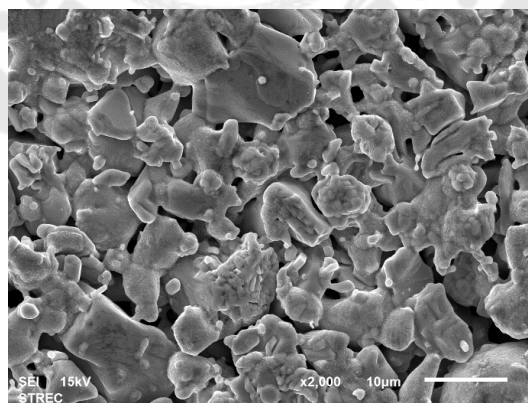
Figure 37 SEM photographs of Y145 + 0.010 Mn₃O₄ at the power magnifications a) 500, b) 1000 and c) 2000



a)



b)



c)

Figure 38 SEM photographs of Y145 + 0.015 Mn₃O₄ at the power magnifications a) 500, b) 1000 and c) 2000

4.3 Energy-dispersive X-ray spectroscopy

4.3.1 EDX of powders reacted

Powders reacted are studied the elemental composition of solid surfaces by energy-dispersive X-ray spectroscopy (EDX) using JEOL (JSM-6610LV) which are used for imaging the surface characteristic of a specimen and analyzed the amount of elements of each superconducting formula. The EDX analysis of Y145 doped with 0.005, 0.010 and 0.015 Mn_3O_4 samples are presented in Table 8.

Table 8 The amount of the elements in many positions

Superconductor	Position	Yttrium	Barium	Copper	Oxygen	Manganese
Y145	1	4.70	16.08	22.43	56.80	-
	2	4.20	16.57	22.51	56.72	-
	3	4.12	15.85	21.58	58.44	-
	4	4.29	16.77	22.50	56.44	-
	5	4.09	16.27	22.07	57.57	-
$YBa_4Cu_5Mn_{0.015}O_y$	1	5.37	16.93	21.50	56.20	0.00
	2	5.27	17.04	21.50	56.18	0.00
	3	4.84	17.06	21.22	56.87	0.00
	4	4.59	17.02	21.69	56.71	0.00
	5	5.04	16.99	21.54	56.43	0.00
$YBa_4Cu_5Mn_{0.03}O_y$	1	4.63	16.78	23.17	55.42	0.00
	2	4.45	17.49	23.21	54.85	0.00
	3	4.56	17.52	22.51	55.16	0.24
	4	4.39	17.03	22.65	55.94	0.00
	5	4.44	17.47	23.28	54.70	0.00

Table 9 The amount of the elements in many positions (Continued)

Superconductor	Position	Yttrium	Barium	Copper	Oxygen	Manganese
YBa ₄ Cu ₅ Mn _{0.06} O _y	1	4.08	17.91	23.44	54.28	0.29
	2	4.78	17.49	23.16	54.58	0.00
	3	4.32	18.12	22.76	54.80	0.00
	4	3.77	17.41	22.93	55.59	0.30
	5	4.26	17.36	22.94	55.25	0.19

In part of analysis composition of all samples, the EDX spectrum are found that the consisted of all samples with Y, Ba, Cu, O and Mn are the different values and no impurity. When we calculate the ratio of the formula by determining yttrium equal to 1. And then, we know that the ratio of Ba, Cu, O and Mn in following Table 9.

Table 10 The ratio of elements in the comparison with yttrium

Superconductor	Yttrium	Barium	Copper	Oxygen	Manganese
Y145	1	3.81	5.19	13.36	-
YBa ₄ Cu ₅ Mn _{0.015} O _y	1	3.39	4.28	11.25	0.00
YBa ₄ Cu ₅ Mn _{0.03} O _y	1	3.84	5.11	12.29	0.01
YBa ₄ Cu ₅ Mn _{0.06} O _y	1	4.16	5.43	12.94	0.04

From Table 9, we also note that the ratio of Ba, Cu, O and Mn represented the inconsistent values of the amount of precursor powders added. It also knows that some region hasn't found the Mn in many position detected in especially the sample of YBa₄Cu₅Mn_{0.015}O_y because of the amount of Mn doped is smaller and may be not distribute in any positions.

4.3.2 EDX of composite materials

Energy-dispersive X-ray spectroscopy (EDX) is used to analyze the elemental composition of materials. The EDX analysis of 0.005, 0.010 and 0.015 Mn_3O_4 samples are presented in the table 9, one can note that each values of Mn_3O_4 is slightly distributed over the entire surface of the granules as points in the micro size range and the elemental analysis into superconductor at a power magnification of 500 which are randomly analyzed five positions on the surface of all samples shown in Table 10.

Table 11 The amount of the elements in many positions

Superconductor	Position	Yttrium	Barium	Copper	Oxygen	Manganese
Y145	1	4.13	16.63	21.05	58.18	-
	2	3.76	16.58	20.75	58.92	-
	3	3.62	16.77	20.62	59.00	-
	4	4.11	16.79	20.76	58.34	-
	5	3.77	16.57	21.04	58.62	-
Y145 + 0.005 Mn_3O_4	1	4.61	17.62	21.74	56.02	0.00
	2	4.33	17.48	22.03	56.17	0.00
	3	4.24	18.95	18.05	58.77	0.00
	4	4.66	17.35	21.69	56.29	0.00
	5	4.88	17.45	20.51	57.16	0.00
Y145 + 0.010 Mn_3O_4	1	4.15	17.53	22.06	55.88	0.39
	2	3.76	17.83	22.03	56.00	0.39
	3	3.68	17.51	22.01	56.47	0.33
	4	3.59	17.69	21.94	56.29	0.12
	5	3.61	17.74	22.55	55.90	0.21

Table 12 The amount of the elements in many positions (Continued).

Superconductor	Position	Yttrium	Barium	Copper	Oxygen	Manganese
Y145 + 0.015Mn ₃ O ₄	1	3.44	17.91	22.31	55.90	0.44
	2	3.97	17.91	22.29	55.47	0.37
	3	3.77	17.69	22.18	56.01	0.36
	4	3.95	18.14	22.65	54.91	0.35
	5	3.52	17.79	22.49	55.86	0.34

The analysis compositions by EDX are found that the consisted of all samples with Y, Ba, Cu, O and Mn are the different values and no impurity. When we compute the ratio of the formula by defining yttrium equal to 1. And then, we know that the ratio of Ba, Cu, O and Mn in following Table 11.

Table 13 The ratio of elements in the comparison with yttrium

Superconductor	Yttrium	Barium	Copper	Oxygen	Manganese
Y145	1	4.30	5.37	15.11	-
Y145 + 0.005 Mn ₃ O ₄	1	3.91	4.58	12.52	0.00
Y145 + 0.010 Mn ₃ O ₄	1	4.70	5.89	14.93	0.08
Y145 + 0.015 Mn ₃ O ₄	1	4.80	6.00	14.91	0.10

From Table 11, we indicate that the ratio of Ba, Cu, O and Mn demonstrated the inconsistent values of the amount of precursor powders added. It also present that some region hasn't found the Mn in many positions detected because of the amount of Mn doped is smaller and may be not distribute in any positions.

4.4 The X-ray diffraction

For the powder X-ray diffraction analysis, the pellets are reground to fine powder and the XRD patterns analysis are investigated. The XRD patterns are carried out at room temperature in $2\theta = 10^\circ - 90^\circ$ range are shown in Figure 39, 40. The characteristic peaks of all samples; the Y145, $\text{YBa}_4\text{Cu}_5\text{Mn}_{0.0015}\text{O}_y$, $\text{YBa}_4\text{Cu}_5\text{Mn}_{0.03}\text{O}_y$, $\text{YBa}_4\text{Cu}_5\text{Mn}_{0.06}\text{O}_y$ in the powders reacted process and the Y145, $\text{Y145} + 0.005\text{Mn}_3\text{O}_4$, $\text{Y145} + 0.010\text{Mn}_3\text{O}_4$, $\text{Y145} + 0.015\text{Mn}_3\text{O}_4$ in the composite materials process, are determined by the full-prop software.

When the peaks of all samples are compared with the peak of Y123 for the investigation of crystal structure. It is mentioned that these peaks corresponding to the peak of Y123 are detected by X-ray diffraction analysis. So that, all samples are presented that the orthorhombic structure.

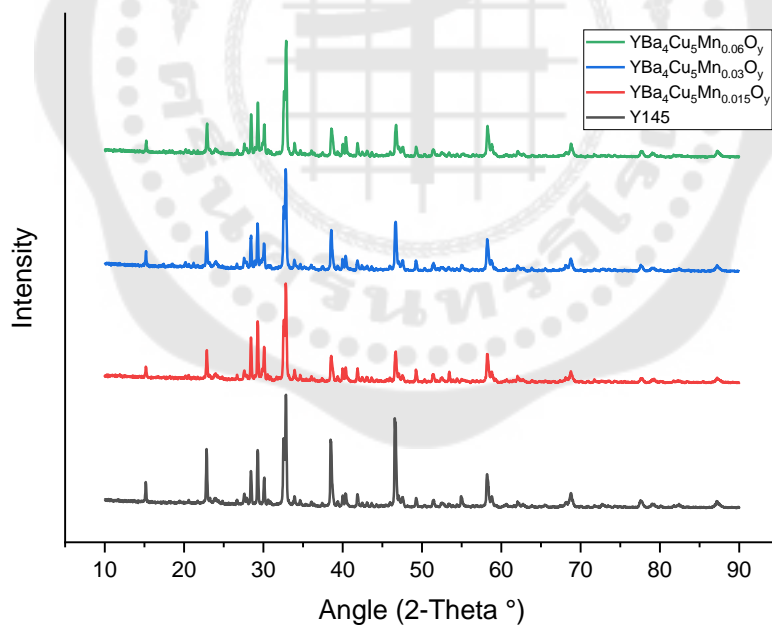


Figure 39 The X-ray diffraction patterns of samples in the powders reacted process.

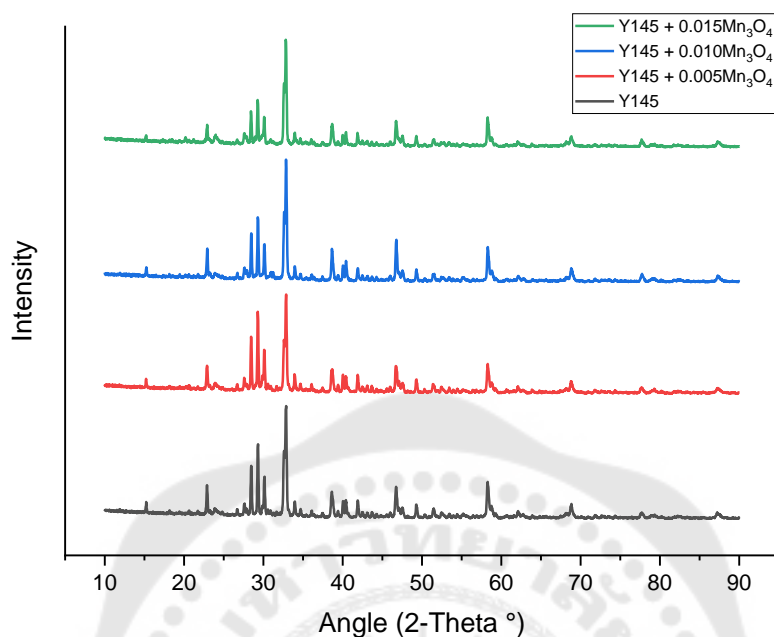


Figure 40 The X-ray diffraction patterns of samples in the composite materials process.

4.5 Iodometric titration

In this study, the Iodometric titration is investigated to determine the amount of Cu^{2+} , Cu^{3+} and oxygen content. The oxygen content O_y has been calculated by using the sum of the oxidation numbers of all samples, they find that $y = 11-x$, where x is the deficiency of samples. The $\text{Cu}^{3+}/\text{Cu}^{2+}$ ratio, oxygen content and the deficiency of all samples are indicated in Table 12. For investigating of all samples, we report that the $\text{YBa}_4\text{Cu}_5\text{Mn}_{0.06}\text{O}_y$ has shown the highest $\text{Cu}^{3+}/\text{Cu}^{2+}$, critical temperature and the lowest percentage of deficiency.

Table 14 This is the oxygen content and deficiency of samples.

Compounds	$\text{Cu}^{3+}/\text{Cu}^{2+}$	Oxygen content (O_y)	Deficiency (%)
Y145	0.170	10.863	1.249
$\text{YBa}_4\text{Cu}_5\text{Mn}_{0.015}\text{O}_y$	0.202	10.921	0.719
$\text{YBa}_4\text{Cu}_5\text{Mn}_{0.03}\text{O}_y$	0.193	10.904	0.870
$\text{YBa}_4\text{Cu}_5\text{Mn}_{0.06}\text{O}_y$	0.222	10.954	0.417
Y145	0.173	10.869	1.188
$\text{Y145} + 0.005 \text{Mn}_3\text{O}_4$	0.201	10.919	0.740
$\text{Y145} + 0.010 \text{Mn}_3\text{O}_4$	0.180	10.881	1.077
$\text{Y145} + 0.015 \text{Mn}_3\text{O}_4$	0.217	10.946	0.491

In Figure 41, the effect of two processes and oxygen deficiency on the critical temperature onset is shown. The relation of these parameter is almost the linear dependence. It also knows that the oxygen deficiency has the small value, which is contributed to the increase of the critical temperature such as the highest deficiency of Y145 has the smaller critical temperature. So we conclude that the critical temperature is inversely proportional to the increasing oxygen deficiency. The ratio of $\text{Cu}^{3+}/\text{Cu}^{2+}$ versus the critical temperature onset of all samples is shown in Figure 42. We indicate that the ratio of $\text{Cu}^{3+}/\text{Cu}^{2+}$ depends on the critical temperature, which is almost the linear dependence. The $\text{YBa}_4\text{Cu}_5\text{Mn}_{0.06}\text{O}_y$ has the maximum $\text{Cu}^{3+}/\text{Cu}^{2+}$ and the Y145 has the minimum that agrees with the highest T_c onset of $\text{YBa}_4\text{Cu}_5\text{Mn}_{0.06}\text{O}_y$ and the lowest T_c onset of Y145. Therefore, we also know that the higher the $\text{Cu}^{3+}/\text{Cu}^{2+}$ ratio is, the higher the critical temperature becomes.

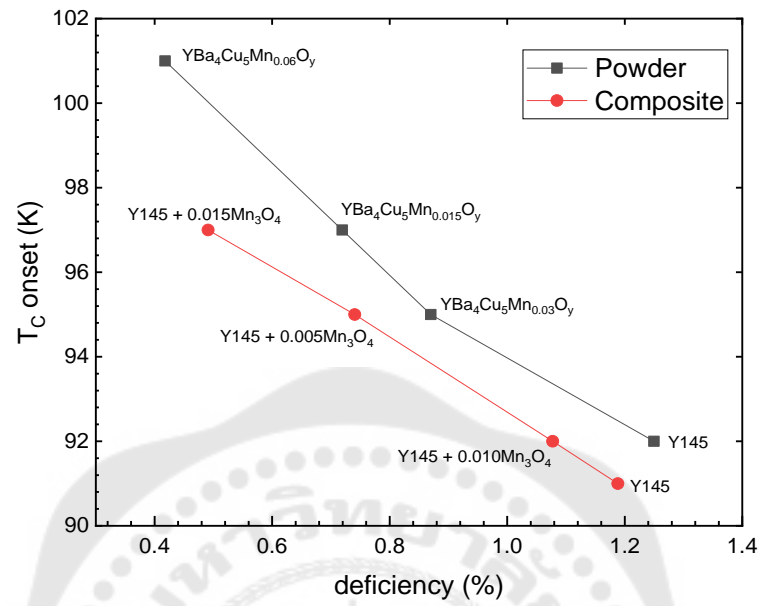


Figure 41 This is the effect of two processes and oxygen deficiency on the critical temperature onset of all samples.

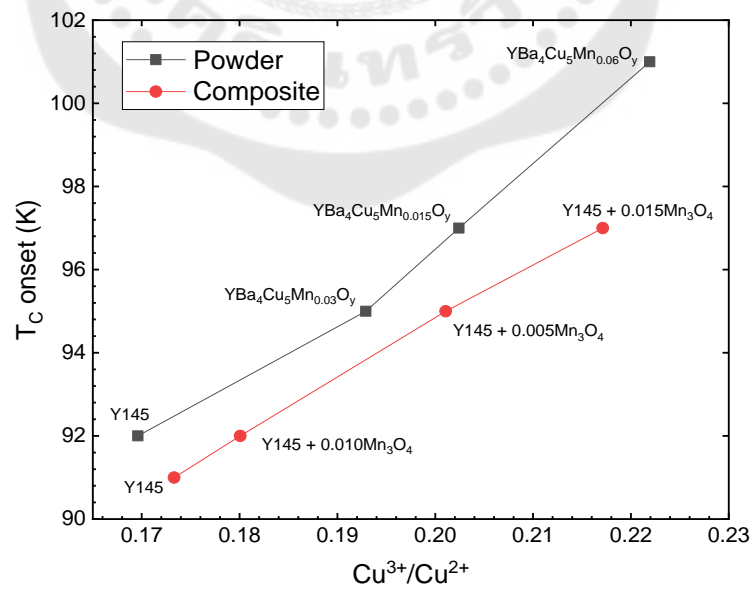


Figure 42 Shows the ratio of Cu³⁺/Cu²⁺ versus the critical temperature onset.

CHAPTER 5

CONCLUSIONS DISCUSSIONS AND SUGGESTIONS

From chapter 4 research results is the results of experiments from the preparation of $\text{YBa}_4\text{Cu}_5\text{O}_y$ and $\text{YBa}_4\text{Cu}_5\text{O}_y$ doping on Mn_3O_4 and investigating the physical properties of Y145 superconductors such as studying the critical temperature with the resistivity measurement by the four-point probe technique, morphology, elements, crystalline structure and Iodometric titration, respectively. Research's results are summarized as follows.

5.1 Conclusions

In this research, we study the influence of Mn_3O_4 composition on some physical properties of Y145 superconductor prepared by solid-state reaction method. We prepare the two processes; the powders reacted process are $\text{YBa}_4\text{Cu}_5\text{O}_y$ and $\text{YBa}_4\text{Cu}_5\text{Mn}_{0.015}\text{O}_y$, $\text{YBa}_4\text{Cu}_5\text{Mn}_{0.03}\text{O}_y$, $\text{YBa}_4\text{Cu}_5\text{Mn}_{0.06}\text{O}_y$ and the composite materials process are $\text{YBa}_4\text{Cu}_5\text{O}_y$ and $\text{Y145} + 0.005\text{Mn}_3\text{O}_4$, $\text{Y145} + 0.010\text{Mn}_3\text{O}_4$ and $\text{Y145} + 0.015\text{Mn}_3\text{O}_4$. These processes are used for the different concentrations (0, 0.005, 0.010, 0.015). The precursor powders include Yttrium Oxide (Y_2O_3), Barium Carbonate (BaCO_3), Copper Oxide (CuO) and Manganese Oxide (Mn_3O_4). These precursor powders are mixed, ground and reacted compounds in a mortar and pestle. And then these powders are calcined and sintered at 950°C and annealed at 550°C .

The resistivity measurements of superconductors by using the four-point probe technique are found that the highest critical temperature is in $\text{YBa}_4\text{Cu}_5\text{Mn}_{0.06}\text{O}_y$ powder reacted sample with T_c onset at 101 K and the lowest is found in pure Y145 at 92 K. In addition, the Y145 superconductors are synthesized by composite materials in the influence of Mn_3O_4 on the critical temperature of samples. The highest critical temperature is in $\text{Y145} + 0.015\text{Mn}_3\text{O}_4$ composite material sample with T_c onset at 97 K and the lowest critical temperature is pure Y145 at 91 K. So that, the Y145 superconductors doped with Mn_3O_4 in the powders reacted process and the composite materials process by the different concentrations can enhance the critical temperature.

And then, it notes that the doping on Mn_3O_4 of the powders reacted process is higher critical temperature than the composite materials process, show that the value of T_C at 101 K which increase T_C significantly in the powders reacted process. While the composite materials process shown slightly critical temperature in the value of T_C onset at 97 K.

In the characteristic of analytical is analyzed by the scanning electron microscopic (SEM) and studied the elemental composition of solid surfaces by energy-dispersive X-ray spectroscopy (EDX). We find that the average grain size in all samples mostly does not change in most samples. The grain size of all samples exhibits large grains randomly oriented in all direction with the presence of slightly pores between the grains. For each doping on manganese oxides, it is shown that manganese oxides are not distributed randomly over the Y145 grains mostly. However, the doping on Mn_3O_4 of Y145 samples are less porosity than no doped. The EDX is found that the ratio of Ba, Cu, O and Mn represented the inconsistent values of the amount of precursor powders added. It also noted that some region hasn't found the Mn in many position detected because of the amount of Mn doped is smaller and may be slightly distribute in any positions.

The investigation of the crystalline structure is used for the X-ray diffraction analysis and determined by the full-prop software. The powder XRD patterns of all samples doped with different concentrations have demonstrated the data. We find that the analysis of the data indicates a predominantly single phase with an orthorhombic structure. There are two composition samples; superconducting compounds and nonsuperconducting compounds. The superconducting compounds are the orthorhombic with a Pmmm space group and nonsuperconducting compounds are $\text{Ba}_2\text{Cu}_3\text{O}_6$ with **Im-3m** space group. When we consider the lattice parameters of all samples with the orthorhombic structure, we also note that the lattice parameters and unit cell volumes of a , b and c for doping on Mn_2O_4 , the a and b parameters are no significant change while c increases slightly as comparing with Y123. The difference between a and b parameters reduces the orthorhombicity and the high value of

orthorhombicity of the Y145 samples is the result of high oxygen content and consequently could give better superconducting properties.

The standard Iodometric titration is determined the amount of Cu^{2+} and Cu^{3+} and oxygen content. For the chemical formula of Y145 samples is $\text{YBa}_4\text{Cu}_5\text{O}_y$ and the chemical formula of Y145 doped with different concentrations in two processes are $\text{YBa}_4\text{Cu}_5\text{Mn}_{0.015}\text{O}_y$, $\text{YBa}_4\text{Cu}_5\text{Mn}_{0.03}\text{O}_y$, $\text{YBa}_4\text{Cu}_5\text{Mn}_{0.06}\text{O}_y$ and $\text{YBa}_4\text{Cu}_5\text{O}_y(0.005\text{Mn}_3\text{O}_4)$, $\text{YBa}_4\text{Cu}_5\text{O}_y(0.010\text{Mn}_3\text{O}_4)$, $\text{YBa}_4\text{Cu}_5\text{O}_y(0.015\text{Mn}_3\text{O}_4)$, respectively. Then, we find that the critical temperature has the relation to the amount of $\text{Cu}^{3+}/\text{Cu}^{2+}$, the deficiency of O_y , c/a ratio of all samples. So we can conclude that the $\text{YBa}_4\text{Cu}_5\text{Mn}_{0.06}\text{O}_{10.954}$ has the highest $\text{Cu}^{3+}/\text{Cu}^{2+}$ ratio equal to 0.222 and the highest critical temperature onset at 101K. While the $\text{YBa}_4\text{Cu}_5\text{Mn}_{0.005}\text{O}_{10.863}$ has the lowest $\text{Cu}^{3+}/\text{Cu}^{2+}$ ratio equal to 0.170 and the critical temperature onset at 92 K. In addition, the critical temperature and the deficiency of O_y is almost the linear dependence. It also indicates that the critical temperature is the inversely proportional to the deficiency. The lower the deficiency is, the higher the critical temperature becomes. And then, it also shows that the difference of T_c onset and T_c offset in each sample slightly decreases as c/a increases. So that, when the superconductors have the highest $\text{Cu}^{3+}/\text{Cu}^{2+}$, which will contribute to increase the critical temperature. It also notes that the ratio of $\text{Cu}^{3+}/\text{Cu}^{2+}$ results on the value of anisotropic and c/a ratio.

5.2 discussion

The preparations of $\text{YBa}_4\text{Cu}_5\text{O}_y$ superconductors doped with different concentrations of $x\text{Mn}_3\text{O}_4$ where $x = 0, 0.005, 0.010$ and 0.015 by solid-state reaction method in two prepared processes; the powders reacted process and the composite materials process. The influence of Mn_3O_4 on some physical properties of Y145 superconductors are measured by the four-point probe technique to find the critical temperature. Firstly, the Y145 superconductor has the critical temperature onset at 91K as corresponding with the research of P.Chainok et.al. Secondly, the Y145 superconductors doped with Mn_3O_4 have higher critical temperature than undoped. in especially, the $\text{YBa}_4\text{Cu}_5\text{Mn}_{0.06}\text{O}_y$ superconductor has the highest critical temperature

onset at 101K and the Y145 + 0.010Mn₃O₄ has the lowest critical temperature onset at 92 K. And then, we find that the results of magnetic micro metal oxides doping on structure and electrical properties of Y145 superconductors are consistent with the research of Salama et.al that the influence of magnetic nano metal oxides, in the doped with Mn₃O₄ by increasing the concentrations. Finally, It also knows that the powders reacted process have higher critical temperature than the composite materials process, demonstrated the value of T_c onset at 101K as comparing with slightly T_c onset at 97 K.

Analysis of the measured X-ray diffraction pattern of the entire sample area shows that the crystal structure of all samples are in the orthorhombic with Pmmm space group. The XRD pattern is also demonstrated the phase of superconductivity in samples. The experimental lattice parameters of this phase are separated in two compositions; superconducting compounds and nonsuperconducting compounds. These are consistent with the analysis of elements, which are shown that some position cannot find the manganese oxides. These manganese oxides are not distributed randomly over the Y145 grains mostly, examined by the electron-dispersive X-ray spectroscopy. However, it also notes that the doping on Mn₃O₄ of Y145 samples mostly does not change in most samples. The grains size of samples exhibits large grains randomly oriented in all direction with the presence of slightly pores between the grains and the space between the grains is narrow.

The investigation of oxygen content in the structure of superconductors are shown that the change amount of Cu³⁺ and Cu²⁺, which are elements of copper in the superconductors. We find that the ratio of Cu³⁺/Cu²⁺ depends on the critical temperature of superconductors. Especially, the Y145 superconductors have a higher Cu³⁺/Cu²⁺ ratio and a higher critical temperature. This results are consistent with the research of Supadanaison et .al found that the higher the Cu³⁺/Cu²⁺ is, the higher the critical temperature found. In addition, it also knows that the amount of Cu³⁺/Cu²⁺ ratio in the superconductors contribute to become the crystal structure of superconductor. Therefore, we also indicate that the Y145 superconductors doped with Mn₃O₄ in the different concentrations, it is evident that the higher the Cu³⁺/Cu²⁺ ratio is, the higher the

superconducting transition temperature becomes. Particularly, the analytical results for the $\text{YBa}_4\text{Cu}_5\text{Mn}_{0.06}\text{O}_y$ sample. It also shows that the increasing of $\text{Cu}^{3+}/\text{Cu}^{2+}$ are enhanced the oxygen content and the critical temperature of samples. And then, the effect of increasing Mn content in the Y145 superconductors are equivalent to that of enhancing oxygen content and the rising of the critical temperature, which influence on the highest anisotropic and c/a ratio.

5.3 Suggestion

The influence of Mn_3O_4 composition on some physical properties of Y145 superconductor prepared by solid-state reaction have to study more physical properties of superconductor such as finding the value of the critical current density (J_c), the hardness or the modulus of elasticity, the phenomenon of Meissner effect, since the Mn-doping is contributed to improve the morphology, which will be able to constitute the analysis results and find out the more precisely relations.

REFERENCES

- Bardeen, J., Cooper, L. N., & Schrieffer, J. R. (1957). Theory of superconductivity. *Physical review*, 108(5), 1175.
- Bednorz, J. G., & Müller, K. A. (1986). Possible high T_c superconductivity in the BaLaCuO system. *Zeitschrift für Physik B Condensed Matter*, 64(2), 189-193.
- Buckel, W. (1991). *Superconductivity: fundamentals and applications*: Weinheim : VCH.
- Chainok, P., Khuntak, T., Sujinnapram, S., Tiyasri, S., Wongphakdee, W., Kruaehong, T., . Udomsamuthirun, P. (2015). Some properties of $YBa_mCu_{1+m}O_y$ ($m= 2, 3, 4, 5$) superconductors. *International Journal of Modern Physics B*, 29(09), 1550060.
- Chainok, P., Sujinnapram, S., Nilkamjon, T., Ratreng, S., Kritcharoen, K., Butsingkorn, P., . Udomsamuthirun, P. (2013). *The preparation and characterization of Y145 superconductor*. Paper presented at the Advanced Materials Research.
- Choy, J.-H., Choi, S.-Y., Byeon, S.-H., Chun, S.-H., Hong, S.-T., Jung, D.-Y., Park, Y.-W. (1988). Determination of the Copper Valency and the Oxygen Deficiency in the High T_c Superconductor, $YBa_2Cu_3O_{7-\delta}$. *Bulletin of the Korean Chemical Society*, 9(5), 289-291.
- Da Luz, M., Dos Santos, C., Shigue, C., De Carvalho Jr, F., & Machado, A. (2009). The van der Pauw method of measurements in high- T_c superconductors. *Materials Science-Poland*, 27(2).
- Epp, J. (2016). X-ray diffraction (XRD) techniques for materials characterization *Materials characterization using Nondestructive Evaluation (NDE) methods* (pp. 81-124): Elsevier.
- Fetter, A. L., & Walecka, J. D. (2012). *Quantum theory of many-particle systems*: Courier Corporation.
- Goldstein, J. I., Newbury, D. E., Michael, J. R., Ritchie, N. W., Scott, J. H. J., & Joy, D. C. (2017). *Scanning electron microscopy and X-ray microanalysis*: Springer.
- Harris, D. C., & Hewston, T. A. (1987). Determination of Cu^{3+}/Cu^{2+} ratio in the superconductor $YBa_2Cu_3O_{8-x}$. *Journal of Solid State Chemistry*, 69(1), 182-185.

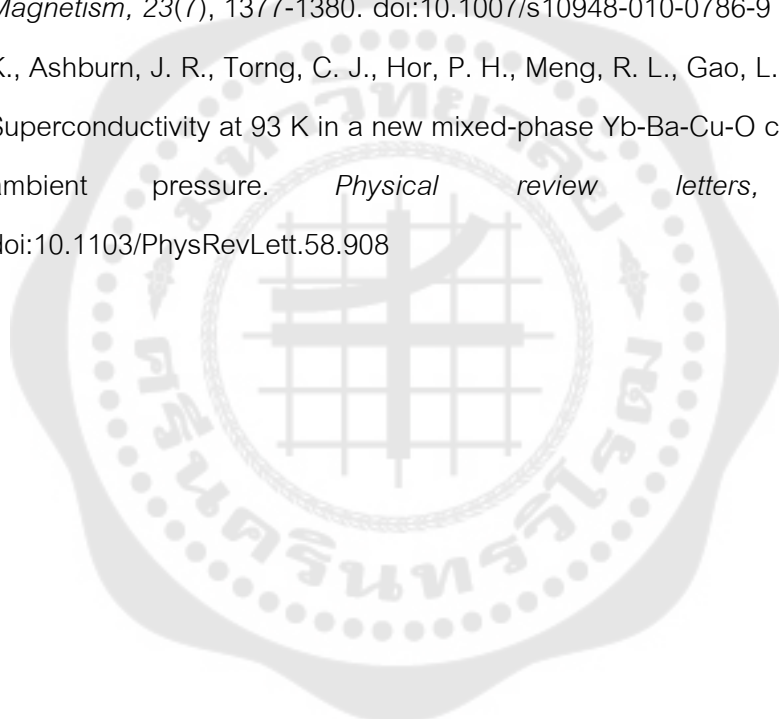
- Harris, D. C., Hills, M. E., & Hewston, T. A. (1987). Preparation, iodometric analysis, and classroom demonstration of superconductivity in $\text{YBa}_2\text{Cu}_3\text{O}_{8-x}$. *Journal of Chemical Education*, 64(10), 847.
- Inkson, B. (2016). Scanning electron microscopy (SEM) and transmission electron microscopy (TEM) for materials characterization *Materials characterization using nondestructive evaluation (NDE) methods* (pp. 17-43): Elsevier.
- Keithley, J. F. (1984). *Low level measurements: for effective low current, low voltage, and high impedance measurements*: Keithley Instruments.
- Kittel, C. (1962). *Elementary solid state physics : a short course*: New York : Wiley.
- Kruaehong, T., Sujinnapram, S., Udomsamuthirun, P., Nilkamjon, T., & Ratreng, S. (2018). *The effect of ti-doped on the structure of γ_{134} and γ_{257} superconductors* (Vol. 18).
- Laphorn, A., Bodger, P., & Enright, W. (2013). A 15-kVA High-Temperature Superconducting Partial-Core Transformer-Part 1: Transformer Modeling. *IEEE Transactions on Power Delivery*, 28(1), 245-252. doi:10.1109/TPWRD.2012.2226478
- Murase, S., Itoh, K., Wada, H., Noto, K., Kimura, Y., Tanaka, Y., & Osamura, K. (2001). Critical temperature measurement method of composite superconductors. *Physica C: Superconductivity*, 357, 1197-1200.
- Omar, M. A. (1975). *Elementary solid state physics : principles and applications*: Reading, Mass., : Addison-Wesley.
- Salama, A. H., El-Hofy, M., Rammah, Y. S., & Elkhatib, M. (2015). Effect of magnetic and nonmagnetic nano metal oxides doping on the critical temperature of a ybco superconductor. *Advances in Natural Sciences: Nanoscience and Nanotechnology*, 6(4), 045013. doi:10.1088/2043-6262/6/4/045013
- Salama, A. H., El-Hofy, M., Rammah, Y. S., & Elkhatib, M. (2016). The influence of magnetic nano metal oxides doping on structure and electrical properties of YBCO superconductor. *Advances in Natural Sciences: Nanoscience and Nanotechnology*, 7(1), 015011. doi:10.1088/2043-6262/7/1/015011
- Sharma, R. G. (2015). *Superconductivity* Vol. 214. Retrieved from 28/03/2019

<http://www.bookmetrix.com/detail/book/b8daf2d7-9419-4516-bb81-c399ddb667ab#citations> doi:10.1007/978-3-319-13713-1

Supadanaisorn, R., Panklang, T., Wanichayanan, C., Kaewkao, A., Nilkamjon, T., Udomsamuthirun, P., Kruaehong, T. (2018). Determination of Cu²⁺ and Cu³⁺ by titration in Y134 and Y145 superconductor. *Materials Today: Proceedings*, 5(7), 14896-14900.

Udomsamuthirun, P., Kruaehong, T., Nilkamjon, T., & Ratreng, S. (2010). The New Superconductors of YBaCuO Materials. *Journal of Superconductivity and Novel Magnetism*, 23(7), 1377-1380. doi:10.1007/s10948-010-0786-9

Wu, M. K., Ashburn, J. R., Torng, C. J., Hor, P. H., Meng, R. L., Gao, L., Chu, C. W. (1987). Superconductivity at 93 K in a new mixed-phase Yb-Ba-Cu-O compound system at ambient pressure. *Physical review letters*, 58(9), 908. doi:10.1103/PhysRevLett.58.908



VITA

NAME Mr. Anongdavone PONCHANTHAI

DATE OF BIRTH 03 December 1991

PLACE OF BIRTH Champassak Province

INSTITUTIONS ATTENDED 2014 Bachelor degree, Physic, Faculty of Education,
National University of Laos

